

Administrative Cover Page: Appendix A.

Unsolicited Proposal Submitted to the Department of Energy

DOE Unsolicited Proposal Manager
Office of Acquisition and Assistance
Mail Stop 921-107
U.S. Department of Energy
National Energy Technology Laboratory
P. O. Box 10940
Pittsburgh, PA 15236
(412) 386-4524

Primary Institution: Doty Scientific, Inc.

Address: 700 Clemson Rd., Columbia, SC 29229

Website: <http://dotynmr.com/>

**Collaborators: University of South Carolina
Departments of Mechanical and Electrical Engineering**

Title: Phase I Development of an Advanced, Intercooled, Ceramic Gas Microturbine

Proposed Duration of Phase I: 12 months

Proposed Amount for Phase I: \$250,000

(Proposed Duration of Phase II, pending successful Phase I, expected to be 60 months)

(Proposed Amount for Phase II, pending successful Phase I, expected to be \$5,000,000)

Requested Phase I Starting Date: August 1, 2003

Type of Business: Small

Principal Investigator: F. David Doty, PhD

Phone: 803 788 6497

email: david@dotynmr.com

Date of Submission: Feb. 20, 2002

This proposal contains proprietary material (identified thus: **), but it may be subjected to external review with standard safeguards.**

Signature of Principal Investigator Date
F. David Doty, PhD, President, Doty Scientific

Signature of Authorized Officer Date
David McCree, Business Administrator

We hereby certify that the applicant has not used nor will use appropriated funds for payment to lobbyists

Phase I Development of an Advanced, Intercooled, Ceramic Gas Microturbine

Abstract

Current-technology recuperated open Brayton cycle Micro Gas Turbines (MGTs) operating off methane, ethanol, kerosene, propane, gasoline, JP-8, or H₂ can achieve total emissions (NO_x + CO + UBC + fine particulates) below 4 ppm but have serious mass, efficiency, and cost challenges. Our experiments, detailed analyses, and simulations establish the basis for enormous advances in this engine that promise to make it superior to both the advanced diesel and fuel cells for numerous applications. The design integrates advanced features in the Lu-Si₃N₄ turbine, 2-stage compressor with intercooling, micro-jet combustor, ultra-high-speed variable-flux generator, ceramic ball bearings, and power conditioning. The dual-spindle compressor will enable high efficiency over a very wide load range, from idle to full power, over a wide range of environmental conditions. The Phase I is expected to include off-design engine calculations and simulations, genetic-based CFD and FEA turbine-blade optimizations, oxidation/recession tests of Lu-Si₃N₄ in exhaust environments, low-NO_x micro-jet combustor optimization, initial spindle designs for a 30 kW demo hybrid, and tests of a model spindle at design rpm. Manufacturing cost analyses will also be an important part of both Phase I and Phase II.

The advanced developments required for the solution proposed herein are expected to have far-reaching applications for numerous power sources, including both hybrid automobiles and off-road generators, where emissions, efficiency, noise, mass, variable-load, and multi-fuel compatibility are important. The design is expected to scale well from 10 to 500 kW, with potential for over 50% system efficiency at 100 kW_E with system mass below 130 kg. The development time frame is expected to be much shorter than is currently projected for economically practical automotive fuel cells.

Key words. Ceramic gas turbine, microturbine, intercooled, low NO_x combustion

Proprietary material throughout proposal identified thus: **.**

Contents

1.0 Identification and Significance of the Challenge and Technical Approach	4
1.1 Introduction	4
1.2 Current Technologies	4
1.3 Advances in R-OBC MGT Technologies	5
2.0 Phase I Technical Objectives	10
3.0 Phase I Work Plan	11
3.1 Analysis, Design, and Optimization of The Intercooled MGT System	11
3.2 The Microturbine Si ₃ N ₄ Expanders	14
3.2.1 The Si ₃ N ₄ Turbine Industry	14
3.2.2 State-of-the-art Turbine Materials	15
3.2.3 Solving the Si ₃ N ₄ Oxidation Problem	15
3.2.4 The Turbine Design	17
3.2.4.1 Solving the Foreign Object Damage (FOD) Problem	17
3.2.4.2 Optimization using Genetic-based Algorithms	18
3.3 The Compressor	18
3.4 The Spindle Bearings	19
3.5 The Spindle Designs	20
3.6 Low-emissions, High-stability Combustion Using Micro-jets	22
3.7 Compact Ultra-high-temperature Recuperators	23
3.8 The Generator and Power Conditioning	26
3.9 The Control System	28
4.0 Phase I Performance Schedule	28
5.0 Related Research and Development	29
6.0 Commercialization Strategy	29
7.0 References	30
8.0 Biographical Sketches	
9.0 Facilities and Equipment	
10.0 Consultants	
11.0 Related Proposals	
12.0 Budget	

Phase I Development of an Advanced, Intercooled, Ceramic Gas Microturbine

1.0 Identification and Significance of the Challenge and Technical Approach

1.1 Introduction. While near-term improvements can be expected in current technologies from standard engineering progress, a bold commitment to an advanced but realistic, science-based power source is required to meet the emissions, fuel type, and fuel mileage challenges of hybrid automobiles for the next century. Because of numerous serious technical, economic, social, and legal issues, projections for the time when fuel cells can begin to make a meaningful contribution to our transportation needs are steadily becoming more – not less – remote.

1.2 Current Technologies. Advanced automotive gasoline engines in the 15-300 kW range (20-400 hp) with advanced catalytic converters achieve relatively low emissions at 30-60% load – often under 70 ppm total CO + UBC + NO_x + fine particulates at 40% load, though tailpipe emissions often increase to 2500 ppm at under 10% load and 1000 ppm at full load [1]. They also achieve 28% shaft efficiency at design conditions, but the prospects for further improvements in either efficiency or emissions are limited. Diesel engines have much better efficiency, and recent progress with very high-pressure fuel injection promises **net system efficiency** η_s above 48% in larger engines at sea level. However, they are rather massive and noisy, and *diesel-compatible catalytic converters for automobiles reduce the high engine emissions by only a factor of two*. Moreover, diesels are not compatible with renewable fuels such as ethanol and hydrogen.

Turbo-generators *below* 300 kW have seen limited commercial success (except for aero auxiliary power units, APUs, which have η_s in the 3-9% range), partially because it becomes difficult to achieve high-efficiency in high-compression-ratio axial-flow compressors at mass flows below ~2 kg/s. There have been a number of well-funded efforts over the past five decades to scale the gas turbine down to the 10-300 kW range with improved efficiency at lower turbine inlet temperature by adding a compact recuperator or regenerator [2-5]. The last decade saw a rebirth of interest in the Micro Gas Turbine (**MGT**) for onsite power generation from companies such as Ingersoll-Rand, Kawasaki, GM/Williams, and Capstone [6,7].

These current off-the-shelf MGTs easily achieve well over two orders of magnitude reductions in both acoustic noise and emissions compared to the diesel engine. They also are multi-fuel compatible (kerosene, methane, ethanol, propane, JP-8, etc.), have lower signatures, and may require less maintenance. However, current MGTs in the 25-150 kW range have rather poor specific mass (11-24 kg/kW_E) and unimpressive efficiency (25-34% at design inlet conditions of 290 K, 101 kPa) that further degrades rapidly for off-design conditions. These current products might tend to dampen enthusiasm for this engine; but this should not be the case when one understands that (1) the poor specific mass of existing MGT's comes primarily from their recuperators, generators, and power conditioning & control (**PCC**) systems, (2) their unimpressive efficiency is due primarily to their low turbine-inlet-temperature (**TIT**), as required by their use of an uncooled superalloy expander turbine, and (3) *dramatic technological advances are now possible in both of the above key areas*.

In Table 1, we compare performance for several small generators of power P_E, for use in hybrids, in: acoustic noise N_A (at 2 m, unenclosed), **net system efficiency** η_s (lower heating value, LHV), **system specific mass** m_{ss} (includes empty fuel tank, engine, generator, and PCC), responsiveness, harmful emissions (ppm, NO_x+CO+UBC+finest), exhaust temperature, lifetime, and cost [7-10].

Engine	P _E	N _A	NO _x +CO+UBC+finest	Fuel	Response Time	m _{ss}	Exhaust Temp.	η_s	Design Lifetime	Cost
	kW _E	dB _A	ppm		s	kg/kW _E	K	%	hours	\$/kW
Stirling	30	68	50	multi	400	28	500	25	40,000	4,000
Current MGT	28	65	4	multi	20	16	530	26	30,000	2,800
Current Diesel	30	90	5000	diesel	4	15	820	28	5,000	500
Advanced Diesel	30	86	2000	diesel	3	9	900	37	10,000	800
PEM Fuel Cell*	30	65	2-3,000	*H ₂	30-200	12	370	38	1,000	8,000
2nd-Generation MGT	30	60	4	multi	3	3.9	490	40	20,000	1,300
3rd-Generation MGT	30	60	5	multi	2	3.6	515	42	20,000	1,500

4th-Generation MGT	100	60	6	multi	3	1.4	532	49	30,000	900
--------------------	-----	----	---	-------	---	-----	-----	----	--------	-----

*The emissions from a PEM fuel cell (or PEFC) with next-generation reformers and catalytic conversion using gasoline or ethanol are expected to be 150 ppm CO, 2000 ppm CH₄, plus some additional UBCs; and the reformers will be very expensive and have short lifetime [11]. Expect for the fuel cells, the above emissions assume no catalytic conversion in the exhaust. Also, note that those fuel-cell plants which have achieved high efficiency (40-60%) and reliability at reasonable cost are extremely massive – 45-90 kg/kW. Fuel-cell engines with mass and reliability suitable for automotive applications do not yet actually achieve the performance listed above in Table 1 [9].

The above costs (except for the diesels) assume production volumes comparable to those of current MGTs – ~300 units per year. (Capstone has been selling MGTs at \$1100/kW, but this is 40% of their actual cost by standard accounting methods.) The cost of the advanced MGTs should drop by a factor of three for production quantities of 10,000 units per year, similar to those of the diesel engines. Of course, in all cases, one can increase efficiency and/or reduce mass at increased cost, but the above numbers represent balanced designs. Note that the unfavorable mass of the PEM fuel-cell system comes primarily from the H₂ storage tank or the massive (and expensive) liquid fuel reformer. And low mass is critical for good urban mileage.

1.3 Advances in R-OBC MGT Technologies. The TIT is the strongest driver of MGT efficiency; and at temperatures above 1550 K, *the new lutetium-bonded silicon nitrides have creep rates in thin sections three orders of magnitude lower than Honeywell's AS800 Si₃N₄ (released in 1999) [12]. We will also show how recession/oxidation rates can be reduced by over two orders of magnitude at temperatures above 1650 K.* High-speed permanent-magnet (PM) generators allow dramatic reduction in the mass of the generator and PCC. For example, we have demonstrated ~97% efficiency from a 50 W generator with a 1-gram rotor at 1,000,000 rpm [13].

We will show in this proposal how a number of recent industry developments (Lu₂Si₂O₇-bonded Si₃N₄, high-speed silicon-nitride ball bearings, **vastly improved oxidation resistance** of Lu-Si₃N₄, and improved CFD software), together with a number of crucial steps we have taken in the past two years (a factor-of-three reduction in recuperator and PCC masses, minimization of Si₃N₄ recession, ultra-low emissions from combustion in the auto-ignition regime, etc.) now point to the recuperated, variable-pressure-ratio, intercooled, MGT as the preferred power source for applications below ~1 MW requiring low emissions, high efficiency, or low signatures over a broad range of environmental and load conditions.

*A very exciting result from our recent CFD simulations was our determination that ultra-low emissions can be achieved in the auto-ignition regime from our novel combustor design. Achieving stability in lean premix combustors (the standard method for low emissions) with air-inlet temperature greater than the autoignition temperature, especially with equivalence ratios below 0.4, has been perceived to be extremely challenging [2, 14]. However, the CFD shows our novel micro-jet concept will provide a robust solution for this regime with **NO_x, CO, and UBC production each well below 1 ppm** – this due primarily to its ultra-short residence time in the miniscule stoichiometric zones.*

Advanced Lu-Si₃N₄, ultra-high-speed generators, our novel oxidation/recession control strategy, microjet autoignition combustor, and superalloy microtube recuperator are enabling technologies for the 45-year-old dream of high-performance, low-emissions MGTs utilizing ceramic turbines and a wide range of available fuels. Several of the less widely appreciated and perhaps counter-intuitive points we will discuss later include:

- A. Uncoated Si₃N₄ turbine oxidation/recession rates are higher by a factor of 15-40 in an unrecuperated gas turbine than in a recuperated gas turbine (with $\eta_x = 0.91$) for the same TIT, fuel type, outlet pressure, and power with the same silicon nitride because of the huge dependence on H₂O partial pressure;
- B. The intercooled cycle not only improves efficiency by reducing compressor load, it also increases the optimum pressure ratio for the highly recuperated cycle, which reduces recuperator, turbine, and even generator masses and thus also reduces system cost and mass.
- C. A quad-spindle design permits a recuperated gas turbine to operate over more than an order-of-magnitude load range with high efficiency and makes it easier to minimize tip clearances and reduce cost;

D. The most practical approach to very-high-temperature recuperators utilizes microtubes, as this minimizes pressure losses and allows materials stresses to be reduced by an order of magnitude compared to those typically encountered in current brazed-foil recuperators;

E. After several minutes of warm-up, an advanced MGT with a compact recuperator can idle efficiently at 3-7% of design power and then accelerate to 80% of full power in 2-6 seconds.

In all phases of our development and design, we address the all-important issue of production cost. Some of the proposed changes will be much less expensive (e.g., system assembly/service labor, ceramic ball bearings, microjet combustor, and PCC), while others (e.g., our MTS recuperator, Si₃N₄ expander turbine) will be more expensive compared to current practice. The most expensive single component of the proposed fourth-generation design will clearly be the recuperator; and, since the design reduces material usage by a substantial factor, the primary factor in its cost is production volume. The numerous advantages of the proposed turbogenerator (ultra-low emissions, high efficiency, low mass, low signatures, stable *electrical* output, fast response) seem to make it ideal for many applications over the range of 5-500 kW. *The modular aspect of our Micro-tube Strip (MTS) recuperator design means that volume production of any size engine will make low-cost superalloy recuperators available for all other sized 4th-generation MGTs.*

While this proposal is by no means a quick-fix approach, a modest-budget demonstration is possible using off-the-shelf components where possible. For example, low-cost aluminum-alloy turbo-charger compressor impellers are available and current-technology MGT recuperators may be used initially. Turbocharger expander turbines, as shown in **Figure 1**, have been in commercial production from a low-creep grade of Si₃N₄ for more than a year.

Table 2 summarizes the relative benefits of the primary technology development issues which strongly affect m_{SS} or η_S for a small (30 kW) MGT. For larger generators, the benefits are a little less.

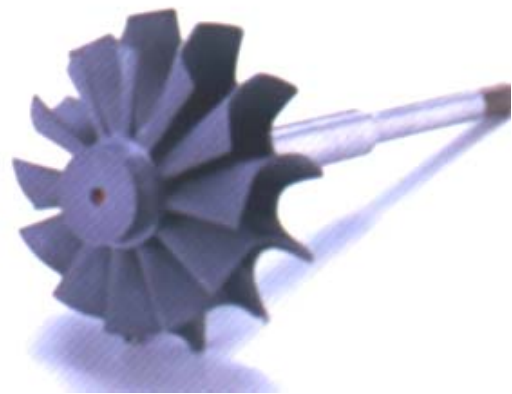


Figure 1. Kyocera has demonstrated production of Lu-Si₃N₄ micro-turbines.

Table 2. Advanced MGT Technology Benefit Summary					
Parameter	Current Technology	Goals Near-term - Long-term	Novel Methods / Advanced Technology	% Near-term Benefit	
				Decrease m_{SS}	Increase η_S
TIT	Bare superalloy 1175 K	Ceramic, 1400 - 1800 K	Adv. Lu-Si ₃ N ₄ turbine; superalloy recuperator	35	26
Compressor optimization	$\phi=76\%^A$, $r=4$ @ 0.2 kg/s	$\phi=80-85\%$, $r=6$ @ 0.2 kg/s	Intercooled radial-flow; extended diffuser	18	16
Recuperator SC, W/kgK	28 W/kgK; high stress	60-90 W/kgK; low stress, etc.	MTS recuperator; microtubes	35	13
Expander optimization	$\epsilon=79\%^A$ @ 0.2 kg/s; $r=4$	$\epsilon=83-88\%$ @ 0.2 kg/s	Two-stage radial-flow; higher r ; robust blades	15	8
Generator	IPM	Ultra-high-speed IPM	Laminated NbBFe rotor inside sleeve	16	4
HF/DC Power conditioning	PWM inverter	Variable frequency	Constant-voltage, variable flux generator	20*	3
Tip Gap	3% of span	1% - 0.7%	Coupled split spindles	0	6
Spindle Bearings	foil-backed air, hydrodynamic	no modes within operating range	Si ₃ N ₄ ball bearings, oil-cooled	8*	2
Signatures, Emissions	65 dB _A noise, 5 ppm NO _x	60 dB _A noise, 2ppm CO+NO _x	Intercooled compressor; Microjet combustor	*	*

^AThe polytropic component efficiencies listed above under "Current Technology" assume conventional blade designs with 1% tip gap. *We do not duplicate benefits that were accounted for in

prior lines. The mass penalty of multiple spindles is negated by its benefit in the generator/PCC from higher rotational frequencies.

Table 2 gives only a glimpse of some of the critical technologies and benefits. Several additional advanced-MGT system design points are: (1) the strongest justification for 2-stage expansion is that it dramatically reduces turbine stresses and thus greatly relaxes defect requirements (Weibull modulus) in the Si_3N_4 turbine; and (2) the four most important factors in achieving high performance over a wide range of loads and environmental conditions are:

- A. The use of advanced, multi-stage, robust, radial-flow turbomachinery;
- B. Ability to control the compression ratio independently of the expander spindle speed;
- C. The ability to obtain high generator efficiency irrespective of the spindle speed and load level;
- D. The use of a high-effectiveness recuperator with reduced exhaust-side pressure drops.

We will show that the past three decades of intense work by a number of well-funded research groups around the world on ceramic gas turbines has unfortunately wound down just when a number of major problems have been solved and others are about to be solved [2, 3, 12, 15-17]. The primary limitations of Si_3N_4 have been: (1) the poor oxidation resistance of earlier grades of Si_3N_4 above 1300 K in conventional (unrecuperated) gas turbines and (2) the poor suitability of Si_3N_4 to axial-flow turbines, where blades require much higher impact strength and vibration tolerance. Also, recall that the strength of ceramics decreases with increasing volume (because of the random nature of defects), and the required turbine volume is proportional to $(P_E/r)^{4/3}$. So *ceramics are much better suited to small turbines*. Our recent analysis shows that an increase of **two orders of magnitude** in lifetime of Si_3N_4 can be obtained above 1350 K from the combination of a number of factors, including (1) one-fourth the H_2O vapor partial pressure in the exhaust for the recuperated MGT compared to the conventional gas turbine, (2) two orders of magnitude increase in viscosity of the glassy inter-granular phases in advanced grades of Si_3N_4 (compared to grade AS800) with an enormous reduction in oxygen diffusion rates, and (3) optimally designed, robust, two-stage radial-flow turbines. The cost of the engineering and production tooling needed for a new size Si_3N_4 turbine for a specific small engine is now relatively minor (~\$250K), and no grinding is needed on the blades following gas-pressure sintering.

Some results of our system analysis and CFD simulations are shown in **Table 3** for (A) the proposed 2nd-generation 30 kW GenSet (4 year development time-frame) and (B) a 4th-generation 100 kW GenSet (8-year time-frame). Here, three successive lines characterize each engine, showing how some of the key parameters change as the engine load goes from maximum to near-minimum load at 1 km (3280 ft) altitude. In Table 3, the recuperator's effectiveness η_x and total normalized pressure drop δ_r are listed, followed by the pressure ratio r and polytropic efficiencies for the compressor ϕ and expander ε , TIT, and rotational frequency f in Hz. Mass-flow rate G , system mass M (including generator and DC PCC), electrical output power P_E , and efficiency η_s are then listed. Naturally, the calculations include allowances for all losses, structure mass, etc. All assume intercooler effectiveness of 60%, recuperator insulation 4.2 cm thick, total electrical output losses of 3%, and compressor inlet conditions of **283 K, 90 kPa**. The engine is optimized for highest efficiency at ~80% of maximum load. The component efficiencies are realistic for near-term developments, though the CFD indicates better efficiency will soon be obtained.

Engine		Recuperator		Compr.		Expander			System, at 1 km Altitude				
#	Load	η_x	δ_r	r	ϕ	ε	TIT	f	G	m_{ss}	M	P_E	η_s
	%	%	%	-	%	%	K	Hz	kg/s	kg/kW _E	kg	kW	%
A	100	91	9.4	5.6	80	82	1400	2060	0.135	3.9	116	30	40
A	25	95.5	9.1	2.5	75	77	1250	1230	0.074	-	-	7.4	32
A	5	97.1	9.4	1.6	66	68	1150	820	0.05	-	-	1.5	14
B	100	92	8.1	7.2	82	84	1670	1670	0.3	1.4	140	100	49
B	30	96.0	8.6	3.0	77	79	1490	1000	0.16	-	-	30	45
B	7	97.5	10	1.8	67	69	1390	670	0.1	-	-	7	29

Essentially off-the-shelf cross-corrugated (CC) recuperator technology can be used for 2nd generation MGTs and preliminary tests of 3rd-generation MGTs, but a substantial federal investment in new heat exchanger production methods is needed to demonstrate the full potential of advanced MGTs. **We have demonstrated micro-tube strip (MTS) recuperators that enable a factor of 2 to 5 reduction in specific mass** (for the same altitude, η_x , and δ_r) and have the potential to go to turbine outlet temperature $T_5=1030^\circ\text{C}$ ($\sim 400^\circ\text{C}$ higher than current commercial compact units) because of enormous reduction in materials stresses [18].

The Japanese Automotive (100 kW, Toyota) Ceramic Gas Turbine Program [2] is probably the closest prior work to our approach. Many of the system differences are discussed elsewhere, but we note below several major differences between our ceramic turbine design and theirs:

- (1) Two-stage expansion allows a factor of two reduction in peak stresses (critically needed for reliability of Si_3N_4) in the turbine for a given TIT and pressure ratio. (Two-stage expansion also gives at least a 4% improvement in ϵ and permits operation at higher r for improved m_{SS} , etc.)
- (2) *Creep rates in current SN282 are 2-3 orders of magnitude lower than in SN252 or AS950.**
- (3) The 9% mechanical loss in the gear box is eliminated by the ultra-high-speed generator.
- (4) The 5% flow leakage from the rotary regenerator and the high-probability of a "foreign" object (from the ceramic honeycomb) are eliminated by using a recuperator.

(*We note that SN282 was developed by Kyocera and Kawasaki as their twin-spool 300 kW program was winding down in 1999, and one rotor test may have been initiated with it. But there were numerous show-stoppers there, not the least of which were the huge thermal stresses in their stator, their choice of axial-flow turbines, severe rotordynamic problems, their use of a ceramic recuperator, abradable shrouds, etc. [19].)

While Foreign Object Damage (FOD) has often been identified as the primary cause of unsatisfactory experiences with ceramic turbines, we do not expect it to be a serious issue in our engine for a combination of reasons (lower turbine stresses, no ceramic regenerator or abradable shrouds, no creep-enhanced crack growth in $\text{Lu-Si}_3\text{N}_4$, more robust turbine blade design, no carbon spalling, etc.) that are discussed in more detail later.

The next closest prior work is the 300 kW intercooled recuperated MGT (with an uncooled superalloy turbine) by Toyo Radiator Company. They reported test data at several inlet temperatures, pressure ratios, and flow rates [20]. Their most complete and unambiguous test and simulation data are presented for the case for $\text{TIT} = 1223 \text{ K}$, $r = 9.0$, and $G = 1.69 \text{ kg/s}$, which gave $P_s = 310 \text{ kW}$ with measured cycle efficiency of 33.8% – in precise agreement with our calculations. Nearly complete data are also provided for the case $\text{TIT} = 1323 \text{ K}$, $r = 7.0$, and $G = 1.51 \text{ kg/s}$, which gave 37.3% cycle efficiency – again in very close agreement with our model.

The major cycle differences between our proposed 30 kW 2nd-generation MGT and the Toyo 310 kW, 1323 K case are illustrated in **Table 4**. We go down the table, starting from the case of all Toyo parameters (which yield 37.6% cycle efficiency), changing one parameter at a time, from the Toyo engine's value to the Doty engine's value, in order of their contribution to efficiency. To clarify, after a modification is listed, it remains in effect through the rest of the table. Hence, the first line is the Toyo case and the last line is the Doty 2nd-generation case.

Even more significant than any of the listed parameters on cycle efficiency is our projected gain in generator/conditioning efficiency. While Toyo obtains only 86%, our experiments give us grounds to believe we will achieve 97% with a relatively modest development effort. This 13% gain is not reflected in the following table. The primary basis for additional gains in subsequent generations is a further increase in TIT, where the practical limit appears to be 1750-1800 K for a 2-stage $\text{Lu-Si}_3\text{N}_4$ microturbine.

Table 4. Effects of changes in primary Brayton cycle parameters on cycle efficiency				
Modified Parameter	Toyo	Doty-2	cycle effic. %	Comments
None	All	none	37.6	(we assume recuperator insulation 7 cm thick)
TIT	1323 K	1400 K	40.0	Still about 400 K below limits for $\text{Lu-Si}_3\text{N}_4$
Recup- η_x	89.5%	91%	42.3	Improved flow uniformity in recuperator
dp-combus.	4%	1%	43.5	CFD-verified, novel, ultra-low- NO_x , low dp combustor
dp-exhaust	8%	4%	44.6	Eliminate exhaust co-gen heat recovery exchanger
IntCooler- η_x	90%	70%	45.3	Drop intercooler effectiveness to reduce dp and mass

r	7	5.8	45.9	more optimum value for reduced pressure losses
φ	78%	80%	47.0	Reduced r and more advanced design
ε	88%	82%	44.1	More realistic value for prelim. 30 kW ceramic turbine

After TIT and recuperator effectiveness, our biggest efficiency gain comes from reducing the pressure loss using the highly optimized ultra-low-NO_x combustor design that we have developed (and carefully verified with advanced CFD). And it is particularly interesting (and perhaps counter-intuitive) to observe the beneficial effects of eliminating the co-gen heat exchanger in the exhaust and reducing the effectiveness of the intercooler. The CFD also indicates we will easily exceed the above listed compressor and expander efficiencies in a 30 kW machine.

At design power levels above ~60 kW, there appear to be at least four distinct challenge levels for the advanced MGT that are summarized below in **Table 5**, with performance for the mobile 100 kW case listed, for example. The first line shows the current-generation 50 kW MGT for comparison. MTS recuperators are required only for 4th and 5th-generation MGTs, where both hot stators are ceramic and the name "Ceramic Gas Turbine" (CGT) becomes fully appropriate. Below 25 kW, it may not be cost effective to advance beyond the 3rd-generation for most applications; and the practical limit for the 25-80 kW range will probably be the 4th-generation.

Gener- ation	max. TIT, K	r (design)	max. T5, K	1st-Stage Turbine		2nd-Stage Turbine		Recuperator, type / material / η_x	m_{SS} kg/kW	η_s %
				Stator	Rotor	Stator	Rotor			
1	1170	3.9	910	MA-956	MA6000	-	-	CC / 347 / 87%	15	29
2	1400	5.4	1070	MA-758	Lu-Si₃N₄	MA-956	MA6000	CC / 120 / 91%	3.2	44
3	1520	6.8	1160	MA-6000	Lu-Si ₃ N ₄	MA-758	Y-Si ₃ N ₄	MTS /317L/ 92%	2.7	46
4	1670	7.2	1220	Lu-Si ₃ N ₄	Lu-Si ₃ N ₄	Y-Si ₃ N ₄	Lu-Si ₃ N ₄	MTS / 120/ 92%	1.4	49
5	1800	7.4	1300	Lu-Si ₃ N ₄	Lu-Si ₃ N ₄	Lu-Si ₃ N ₄	Lu-Si ₃ N ₄	MTS / 230/ 93%	1.2	51

The obvious question that begs to be answered whenever breakthrough claims of enormous importance are made in a mature field is, "Why hasn't one of the established companies (Capstone, Garrett, Ingersoll-Rand, Solar, Sunstrand, Cummins, GM/Williams, Caterpillar) or some other research group already taken your approach if it is so much better?" There are several components to the answer. First of all, each of the established MGT companies has a large, vested interest in system designs and analysis methodologies that have changed relatively little for many years. (Honeywell is now interested only in *unrecuperated* axial-flow turbines, which have been shown to be ill-suited to ceramic blisks and blades [3, 16, 21], partially because of their low impact strength, but even more so because of oxidation issues.) Secondly, the following technologies have only very recently become available:

1. Near-net-shape sintering of low-recession/oxidation, ultra-low-strain-rate silicon nitride;
2. Highly accurate CFD codes with genetic-based turbomachinery optimization algorithms;
3. Ultra-high-speed silicon-nitride ball bearings;
4. High-efficiency, wide-range, ultra-high-speed electric generators.

Thirdly, there are the funding-program-related issues. The Integrated High Performance Turbine Engine (IHPTET) Program (involving DoD, Honeywell, GE, NASA, and others) is focused almost exclusively on propulsion engines, and their minor turboshaft work is for helicopter applications above 1 MW. What little MGT funding that has been available (Advanced Turbine Systems (ATS) program at DOE, DOE Renewables, Next Generation Turbine (NTS) program at DOE, DARPA's nano-scale power, etc.) has been directed either at incremental improvements in conventional designs (Solar Turbines, Allison, Capstone, Ingersoll-Rand, etc.) or in radical MEMs concepts [DARPA/MIT, 22] that have very recently been shown to be impractical. Also, there has been wide-spread emphasis on fuel cells and advanced batteries for the past decade, which has diverted most other power-technology funding.

Finally, solutions have not previously been known for the following challenges, which are critical to the advanced MGT but (especially items 4-6) are less important to the other programs:

1. Effective control of recession/oxidation in Si₃N₄ to 1800 K – a 650 K increase;

2. An effective solution to the Foreign-Object-Damage problem in Si_3N_4 turbines;
3. Spindle designs compatible with the thermal stresses from utilizing ceramics with superalloys;
4. Ultra-compact, low-pressure-drop, cost-effective, superalloy recuperators;
5. Stable, low-emissions combustion in the (required) auto-ignition regime;
6. Control strategies permitting very high efficiency from idle to full power in microturbines.

Our recent work has established that practical solutions appear feasible for the above enabling technologies. We note that over 30% of the cost of current MGTs comes directly from the manufacturing complexities associated with spindle designs that are still influenced heavily from 60 years of aero-jet practice with large axial-flow machines, where minimization of engine mass is more important. Our approach recognizes that simplification of assembly and disassembly is extremely important, and the only component of engine mass that really needs to be minimized is that of the ceramic components.

A business question needing a direct answer is, "How can a small firm expect to succeed where established competitors are likely to be failing soon?" (Capstone's stock is now worth ~1% of its value of 3 years ago [7].) One thing is very clear: the MGT will never compete satisfactorily without 2-stage Lu- Si_3N_4 turbines, intercooled compression, and advances in combustor, spindle, generator, and ultra-compact recuperator technologies. But even with an enormous technical edge (refer again to Tables 1 and 2) and seven years of experience manufacturing Si_3N_4 microturbines, a small firm still faces many challenges. It seems that the most promising approach is to focus on developing effective manufacturing processes and rely on a combination of proprietary technology, patents, and the industry's aversion to innovation to give us enough time to establish a leadership position in the field of advanced MGTs. Our ability to effectively manage R&D, manufacturing, and sales has served us well over the past twenty years with many highly technical products in the face of tough competition. This infrastructure at Doty Scientific should be quite adequate for our small-scale entry into premium military and civilian applications with Advanced MGTs. With our expertise, the world's first reliable Ceramic Gas Turbine, in the form of a 30 kW GenSet suitable for a small hybrid, appears to be practical in the near term with a relatively modest effort. As we establish the enormous commercial potential of Advanced CGTs, numerous other business options will present themselves.

Finally, we note the urgency of the task of pursuing sound avenues toward practical solutions to the transportation crisis our nation will face in a mere ten years, when we find domestic oil and gas sources largely depleted and are forced to rely almost completely on imported, synthesized, or renewable transportation fuels – all of which are likely to be at least twice as expensive as current transportation fuels. Recent appraisals of fuel-cell technology suggest that ten years from now it will still be at least five times as expensive, both in initial capital outlay and in operating costs per mile, as current diesel engines [11]. As the PEFC has been in use and under continual development for 45 years and fuel cell companies are now going bankrupt at record rates, the prospects for substantial progress in cost reductions in less than two decades do not appear very probable. Moreover, practical production of hydrogen for at least the next three decades will have efficiency less than 50% and will release enormous amounts of fossil CO_2 plus other pollutants [9]. The advanced, intercooled CGT, on the other hand, is a novel and practical cycle that appears to have real potential for higher efficiency, much better compatibility with renewable fuels (such as cellulosic ethanol and bio-kerosene), much lower emissions (especially CO_2), and true compatibility with the requirements of the transportation sector.

2.0 Phase I Technical Objectives

The majority of the Phase I effort will be directed toward performing detailed analysis and preliminary design of a 30 kW Recuperated Open Brayton Cycle Micro Gas Turbine (R-OBC-MGT) for operation off kerosene that fits within the space constraints of a small hybrid automobile and easily meets any anticipated environmental and safety requirements for the next century. Also, several experiments will be carried out to establish feasibility of the key technical issues.

2.1 Perform preliminary analysis and initial design of a 30 kW 2nd-Generation MGT.

- 2.1.1 Further develop R-OBC MGT system optimization software.
- 2.1.2 Show that $\eta_s > 39\%$ and total mass less than 130 kg can be expected in early prototypes.
- 2.1.3 Use CFD with conjugate heat transfer (CHT) to design an intercooled 2-stage compressor.
- 2.1.4 Perform off-design system analysis and show that $\eta_s > 30\%$ is expected at 25% load.
- 2.1.5 Show that emissions, mass, safety, and lifetime should easily meet all requirements.

2.2 Combine CFD, oxidation/recession studies, and FEA to arrive at a manufacturable Lu-Si₃N₄ turbine and spindle design for rotor tip speeds above 600 m/s at T₄ > 1650 K.

- 2.2.1 Experimentally evaluate oxidation/recession in several advanced silicon nitrides at 1400 K.
- 2.2.2 Show that turbine lifetime greater than 20,000 hrs can be expected up to 1520 K TIT.

2.3 Design and build first model of 1st-stage expander spindle.

- 2.3.1 Test several different Si₃N₄ ball bearings in high-speed test apparatus up to ~180,000 rpm.
- 2.3.2 Complete full-scale preliminary design of 1st-stage expander spindle with Lu-Si₃N₄ turbine mounted on a superalloy shaft with Si₃N₄ ball bearings, oil seals, thermal insulation, etc.
- 2.3.3 Fabricate first model of expander spindle with a reduced-diameter titanium approximation of the Si₃N₄ turbine suitable for bearing tests at 300 K at 20% beyond final design rpm.

2.4 Perform detailed CFD analysis of micro-jet low-NO_x combustors.

- 2.4.1 Show that fully stable auto-ignition combustion is expected over full range of conditions.
- 2.4.2 Show that total NO_x+CO+UBC+finest is expected to be less than 5 ppm over full range.

2.5 Qualify vendors of a suitable recuperator based on commercial technology.

2.6 Perform preliminary analysis and design of the PCC system.

- 2.6.1 Show that efficiency >98% can be expected from an ultra-high-speed generator.
- 2.6.2 Explore novel variable-flux, constant-voltage, ultra-high-performance generator concepts.
- 2.6.3 Perform detailed FEA on several variable-flux, constant-voltage generator designs.
- 2.6.4 Determine scope of simulations for development of A-MGT optimal-control strategies.

2.7 Devise a preliminary system layout compatible with space in a small hybrid vehicle.

2.8 Write Phase I Final Report and Phase II Proposal.

Without the ability to fine-tune r to adjust for minute component variations, there can be an enormous spread in engine performance. For this reason, currently available 30 kW MGT's are specified with an efficiency range greater than $\pm 12\%$ (e.g., 24-30%) under specified conditions, despite very exacting standards on component manufacturing. Our additional control allows for improved efficiency over a wider range of loads, conditions, and component variations.

For pressure ratio r above ~ 4 , the efficiency of the *recuperated* Brayton cycle without intercooling often decreases with increasing r (though the opposite is true for the *unrecuperated* cycle [19]), but the size and cost of the recuperator decrease. (In some cases the optimum r is as high as 8 [25]. There are a number of factors – foremost among them being η_x , T_4/T_1 , altitude, and δ_r .) Current MGTs operate at $r \approx 4$. For the proposed 30 kW 2nd-generation engine, operation will extend from $r \approx 1.3$ to 7, depending on power level and altitude.

For conceptual purposes, we begin by looking at the single-stage *Closed* Brayton Cycle (CBC), as illustrated in **Figure 3**. With perfect gases (C_p independent of temperature) and without intercool or re-heat, the efficiency is given by the following [19, 26]:

$$\eta_s \equiv \frac{\eta_H \eta_E (E \tau - C)}{\tau [\eta_x (C + E) - C]} \quad [1]$$

where η_E is the generator efficiency, η_H is the heater efficiency, $\tau = T_4/T_1$, $E = (T_4 - T_5)/T_4$, and $C = (T_2 - T_1)/T_1$. The recuperated *open* Brayton cycle is very similar except that (1) the heat rejection occurs external to the engine (without an exchanger) in the infinite atmosphere, and (2) heat addition also occurs without an exchanger via internal combustion. While the above equation lacks some transparency, its beauty lies in its explicit dependence on T_4/T_1 and its absence of explicit dependencies on C_p or γ (C_p/C_v). We can further write, to first order:

$$E = 1 - r(1 - \delta_r)^{(1-\gamma)\varepsilon/\gamma} ; \quad C = r^{(\gamma-1)/\gamma\phi} - 1 \quad [2, 3]$$

where the values of γ above are its mean values in the expander and compressor respectively and δ_r is the normalized pressure drop in the ducts and recuperator – i.e., $\Sigma \delta p/p_0$, where p_0 is the total pressure at the point where the loss is occurring. It turns out that even though C_p increases by 14% in going from 350 K to 1250 K and γ decreases from 1.399 to 1.334, eq. [1] remains fairly accurate for the single-stage CBC, ignoring leakage, bearing, and windage losses and properly accounting for all external heat leaks in η_H .

It should be pointed out that mistakes have often been made in the proper calculation of δ_r . When it is sufficient to assume that all of the pressure losses occur at two pressures (the tube-side and shell-side recuperator pressures), a clearer (and more accurate) expression for E is

$$E = 1 - r_E^{(1-\gamma)\varepsilon/\gamma}, \quad [4]$$

$$\text{where} \quad r_E = (rp_1 - \delta p_t) / (p_1 + \delta p_s). \quad [5]$$

Here, p_1 is the compressor inlet static pressure, δp_t is the sum of the air-side (tube-side) recuperator and combustor pressure drops, and δp_s is the exhaust pressure drop. From eq. [5] it is clear that δp_s is more significant than δp_t by the factor r , which implies that the exhaust-flow (cross-section) area in the recuperator should exceed the inlet-air flow area by roughly the factor r . *One of the inherent limitations in a regenerator is that these flow areas are necessarily equal.* Also, they are usually nearly equal in stamped-foil-type primary surface recuperators. They can be fully optimized only in a (micro) shell-and-tube recuperator.

Now consider the open cycle with vaporized kerosene ($\sim C_{11}H_{24}$) fuel, which has a heat of combustion Q_C of 4.8×10^7 J/kg. For $\eta_x = 0.91$ and the expected 5% total heat leak, T_3 will be ~ 78 K below T_5 , so $(T_4 - T_3)$ is ~ 480 K at $r = 5.6$ for $T_4 = 1400$ K and $\varepsilon = 0.82$. Since C_p is ~ 1150 J/kgK for the mixture at the mean temperature in the expander, the mass fraction of fuel needed for combustion at point T_3 to raise the temperature 480 K is ~ 0.012 , corresponding to an equivalence ratio of only 0.18. Very similar ratios are obtained for JP-8, ethanol, and gasoline. Clearly, very lean-burn conditions occur for all fuels, which allows us to approximate the exhaust in the open cycle

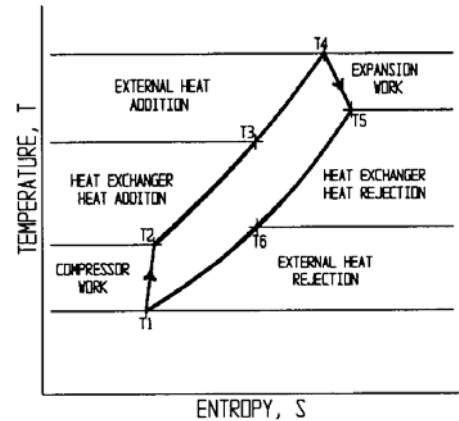


Figure 3. TS diagram for the recuperated single-stage CBC.

as air. Moreover, expander mass flow is only 1% greater than compressor mass flow, so eq. [1] is fairly accurate for the single-stage R-OBC with the same assumptions as for the above CBC.

The TS diagram for the 2-stage, intercooled cycle is shown in **Figure 4**. It has become standard to report LHV efficiency (lower heating value, enthalpy of water vapor in exhaust is ignored). For this cycle (assuming lean combustion), it is quite accurately given by the following:

$$\eta_s = \frac{0.995 \eta_E G C_{PE} [(1 - \lambda)(T_4 - T_5) - (C_{PC} / C_{PE})(T_2 - T_{1B} + T_{2A} - T_1)] - P_B}{G C_{PE} (T_4 - T_3) + P_{HL}} \quad [6]$$

where G is the expander mass flow, C_{PE} and C_{PC} are the mean specific heats in the expander and compressor respectively, λ is relative flow leakage (compressor and turbine seals), P_{HL} is the total heat leak power (primarily through the hot-duct and recuperator insulation), and P_B is the bearing and windage power loss. ("Windage" refers to all gas-related losses not accounted for in either λ , δ_r , ϕ , or ε .) Internal and conjugate heat leaks are assumed properly manifested in ϕ and ε . Equation [6] also assumes the pressurized liquid fuel is first preheated to T_6 (below its boiling point) with waste heat from the recuperator exhaust (T_6). Then, the liquid fuel is boiled and heated to approximately $(T_3 + T_6)/2$ using ~1% of the expander exhaust (diverted from the recuperator at T_5). The vaporized fuel is then injected into the air (at T_3) in the combustor. The numeric coefficient (0.995) corrects for the irreversible aspect of the fuel boiling. The HHV efficiency (higher heating value, including the latent heat of the water vapor in the exhaust at T_6) for light distillate fuels is given by changing this coefficient to 0.97.

The above equations form the heart of the cycle calculations in our Intercooled OBC model software. The recuperator and intercooler are first modeled separately in a way that makes it easy to predict their mass, η_x , δp_s , and δp_t as a function of operating conditions; and a minimum number of characteristic parameters from this model are then inserted into the OBC model. The component efficiencies ϕ and ε , are calculated in agreement with standard models. Simple models for the mass of the generators, PCC, turbomachinery, combustor, and thermal insulation, are also included. Key system parameters and performance measures for the system are then calculated for various conditions. To a first approximation, T_3 , for example, with no heat leak, is simply

$$T_3 \cong T_5 - (1 - \eta_x)(T_5 - T_2) \quad [7]$$

but several corrections, especially in the definition of "apparent effectiveness", are needed for highest accuracy in determining T_3 , T_{2A} , and hence, η_s . Our software has been validated from published data on current microturbines (especially, the Capstone and Ingersoll products), but the component efficiency models still need considerable refinement from extensive CFD simulations of optimized components under off-design conditions. Also, some further development of the software is needed to make it easier to use and have better integration of the various components.

We note that one of the more important aspects of the system calculations is the recuperator performance. We find it most convenient to calculate its mass and effectiveness from a velocity-dependent *Specific Conductance* (SC, heat transfer per mass per mean temperature difference between the counterflowing streams, W/kgK) [18, 27], though others have recently used other normalized metrics for a number of available core geometries [28]. Commercially available nickel-brazed cross-corrugated recuperators with $\delta_r = 10\%$ achieve ~28 W/kgK – when the mass for the SC calculation includes the

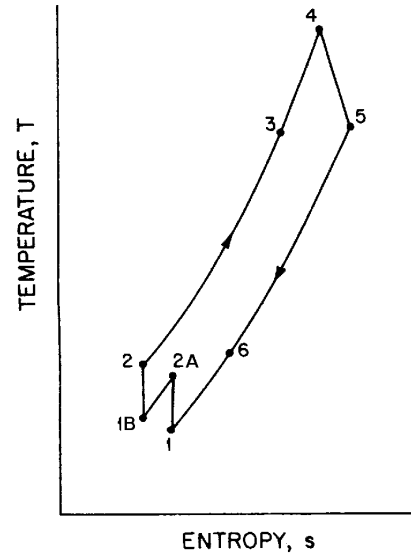
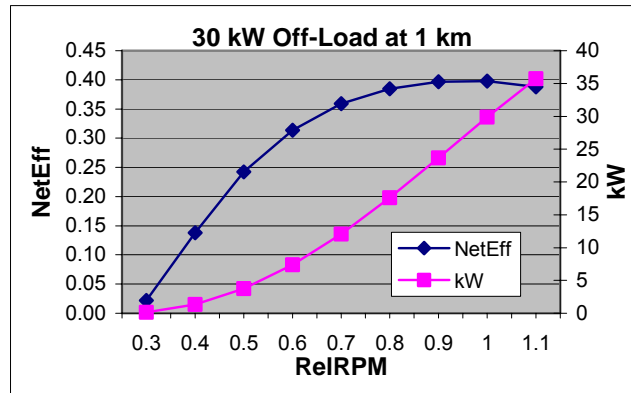


Figure 4. TS diagram for the intercooled recuperated Brayton



manifolding and ducts but not the external insulation and enclosure, which are handled separately in our model. **The complete model will be addressed in more detail in the Phase I Final Report.**

We expect to limit TIT (T4) to 1400 K (still 225 K above current MGT's), largely because of the cost-driven decision to use an advanced superalloy (MA6000) turbine for the second-stage expander initially. As the load and hence r drop, the TIT is deliberately reduced to keep T5 within the allowable limits of the second-stage expander and recuperator. **Figure 5** (above) shows expected off-load performance of the proposed 2nd-Generation MGT at 1 km altitude.

Finally, note that going from single-stage to 2-stage compression and expansion helps not only η_s but also m_{SS} . The primary justifications for two-stage expansion are (1) the factor-of-two reduction in blade stresses at a given r (which is critical for the safety margin needed for a ceramic turbine and higher TIT), and (2) the substantial improvement in mean ε that is realized, primarily because the first stage expander performance is now measured by total-to-total efficiency (which is typically 7 points higher than total-to-static in small radial-flow expanders), as its exhaust does not need to be diffused.

3.2 The Microturbine Si_3N_4 Expanders. Increasing the turbine inlet temperature is a major challenge: the sonic velocity increases, so the tip speed and stresses must increase, but the material weakens and erosion accelerates. Transpiration-cooled, thermal-barrier-coated, single-crystal, superalloy blades seem out of the question below ~ 1 MW, so the primary avenue for progress in efficiency is to switch from superalloy to silicon nitride. The data show the latest Lu-bonded silicon-nitride will now permit 22% higher tip speed at 1800 K than the best superalloys (uncooled) will permit at 1230 K! Our simulations using the most advanced CFD software available (pre-conditioned density-based unsteady RANS with genetic-based optimization [29]) indicate 78-87% polytropic expander efficiency can be achieved over an order-of-magnitude load range at up to 1800 K for readily manufacturable small Si_3N_4 turbines if the rotational rate is properly controlled in a two-stage mixed-flow turbine for total expander pressure ratios up to ~ 7.5 .

We have extensive experience in producing all-silicon-nitride micro-turbine-driven sample spinners (see **Figure 6**) for nuclear magnetic resonance (NMR) of solid samples (where a spinning technique permits spectral line-narrowing). We manufacture NMR probes for use at temperatures up to 1100 K and rotational rates up to 27 kHz (1,600,000 rpm) [30-33]. So we are keenly aware that diamond grinding of silicon-nitride is typically five times more difficult and costly than diamond grinding of either partially stabilized zirconia (PSZ), superalloys, or most silicon carbides.

The cantilevered radial-flow blades used in our NMR products, while ideally suited for the 20-200 W_s range below 1100 K [13, 30, 31], are less optimum above ~ 1 kW_s , where mixed flow, with conventional twisted blades, permits much lower blade stresses and higher polytropic efficiencies. Major advances in gas-pressure-sintered turbines from ultra-low-creep oxidation-resistant grades of silicon-nitride in the last two years should now permit tip speeds over 720 m/s in high-efficiency, mixed-flow Si_3N_4 expanders at 1700 K [2].

3.2.1 The Si_3N_4 Turbine Industry. The last three years have witnessed a tumultuous slowdown in the technical ceramics industry, and the principal developers of Si_3N_4 sintering processes (Kyocera, Ceradyne, Allied/Honeywell, Kawasaki, Permascand, ACC Cerama) have all adjusted their business plans in response to economic realities. Honeywell no longer produces any silicon-nitride parts except for internal use. Kawasaki ended their ceramic MGT program in 1992, and their multi-stage axial-flow ceramic-gas-turbine program was killed in 1999. Norton (now part of the French company Saint Gobain) got out of silicon-nitride turbines in 1995. CoorsTek and Corning no longer make any silicon-nitride parts. Ceradyne seems to be the *only* remaining, major U.S.-based source of demanding Si_3N_4 parts (from raw powders) other than ball bearings, and they have apparently never made turbines. (Javelin 3D, Ceralink, and perhaps others make some small, simple parts.)

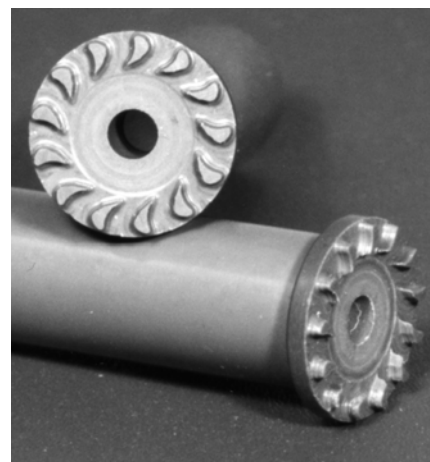


Figure 6. 80 W_s , 0.6 g/s, 1100 K, 5×10^5 rpm, 40% efficiency, Si_3N_4 air turbines used in Doty NMR MAS products.

Kyocera appears to be the *only* firm (world-wide) still producing Si_3N_4 mixed-flow turbines (as shown in Fig. 1) for commercial purposes. Clearly, Kyocera's unique ability to produce high quality mixed-flow turbines from a number of advanced grades of Si_3N_4 (including the new, ultra-low-creep Lu-based grades with excellent oxidation resistance) makes them the only viable option for the first-stage expander turbine at this point in time.

3.2.2 State-of-the-art Turbine Materials. Very effective methods for high-quality densification of silicon nitride without glass encapsulation and HIPing have become well established in the open literature over the past two years. With the proper preparation techniques, binder, plasticizer, and dispersant, the addition of 3-8% sintering aids (usually a combination of Y_2O_3 , La_2O_3 , and Al_2O_3) allows densification and predictable shrinkage in near-net-shape moderate-pressure gas sintering (3 hours at 1800-1900°C in N_2 at 1-2 MPa) [34, 35]. With high-quality silicon-nitride powders (oxygen below 0.2%), the parts routinely achieve bending rupture strength over 750 MPa at temperatures up to 1100 K, very high fracture toughness ($\text{MPa}\cdot\text{m}^{0.5}$), and Weibull modulus above 15 [36]. (The highest Weibull modulus has reportedly been obtained using La_2O_3 as the primary sintering aid [37].) With the proper sintering cycle, a bimodal microstructure is obtained which enhances toughness and high-temperature creep strength [16, 35, 38].

Substitution of Lu_2O_3 (which forms a $\text{Lu}_2\text{Si}_2\text{O}_7$ phase) for most or all of the sintering aid results in slightly reduced RT strength, Weibull modulus, and shrinkage accuracy; *but the strain rates above 1550 K are reduced by several orders of magnitude. Moreover, oxidation resistance is also dramatically improved* [39]. This is the basis of the recent Kyocera grades SN281 (HIP'd) and SN282 (sintered).

Figure 7 illustrates approximate stress limits for 0.6% cumulative strain (or rupture, whichever occurs first) in 10,000 hours as a function of temperature for several turbine materials: Kyocera's SN282, Honeywell's grade AS950 (La-based sintering aid), one of the best conventional nickel-based wrought superalloys Udimet 710, and one of the best oxide-dispersion-strengthened (ODS) mechanically alloyed (MA) superalloys, MA6000. (The superalloys, of course, have 2.3-2.6 times the density of the silicon nitrides). The data here are for very thick material sections. The formulation and process used in AS800 and AS950 to enhance Weibull modulus in thick sections result in creep rates in the surface layer (to several millimeters depth) in the as-fired condition that are **higher by factors of 10-30** than exist deeper within the material [36]. Hence, the Lu-based materials are probably preferred in small machines for TIT as low as 1150 K, especially because of their superior oxidation resistance, as discussed shortly.

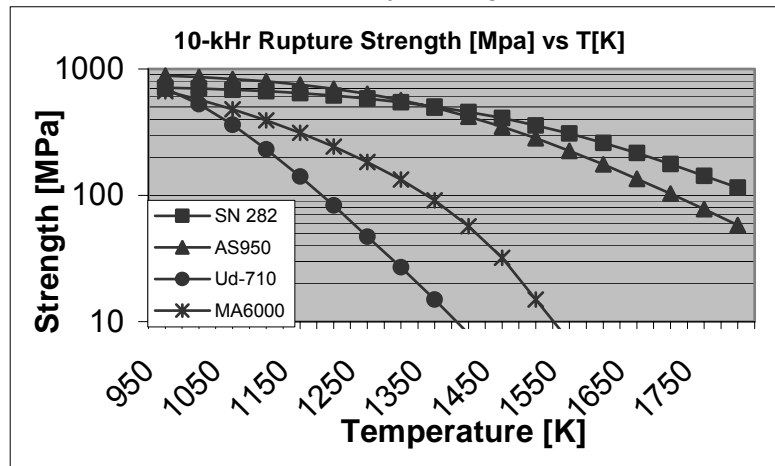


Figure 7. Rupture strength (neglecting oxidation) for two of the latest silicon-nitrides and two nickel-based superalloys.

Continuous-fiber-reinforced ceramic composites (CFCC), especially the SiC/SiC materials, have received a lot of attention; but they are currently achieving only 150 MPa 100-hr rupture stress in air at 1570 K [16, 40, 41], which is more than a factor of three short of competing with the latest gas-sintered Lu- Si_3N_4 . The past four years has seen the gap in long-term rupture strength between SiC composites and sintered Si_3N_4 only widen in long-term rupture strength – at least up to 1700 K. Moreover, the impact strength of Si_3N_4 is at least a factor of three greater than that of the best SiC composites. So not only is Lu- Si_3N_4 clearly the best material for uncooled turbines today, there seems to be little chance that it will be superseded for at least several decades.

**** **3.2.3 Solving the Si_3N_4 Oxidation Problem.** All grades of Si_3N_4 begin experiencing some material loss/recession in high-velocity exhaust streams above 1200 K, and the rates may become rapid above 1900 K. The mechanisms are only recently beginning to be well understood.

Erosion of uncoated AS800 (La-Y- Si_3N_4) in exhaust streams appears to be low enough for lifetimes of ~10,000 hours for the first-stage blisk in a 300-500 kW APU using a three-stage axial turbine, the Honeywell 331-200/250 [3]. This is an unrecuperated engine (net shaft efficiency of

~30%) operating at 1255 K TIT with a pressure ratio of 8.8 from a two-stage radial compressor. So perhaps one would expect only a few hundred hours lifetime from uncoated AS800 in a 30 kW machine of similar design for 1400 K TIT. Fortunately, there are a number of measures that can be taken which should enable two orders of magnitude improvement in the lifetime of silicon-nitride turbines at 1400-1800 K. These measures, which we address briefly below, **and will be addressed in more detail in the Phase I Final Report**, are:

1. Minimize the H₂O and particulate content in the exhaust stream;
2. Operate at lower pressures and relative velocities;
3. Use a high-purity Lutetium-based grade of Si₃N₄;
4. Optimize the geometry to minimize flow velocities very near the surface at the edges.

**** **Minimize H₂O, SO_x, and particulates in the exhaust.** For silicon nitrides and silicon carbides, recession of the protective oxide film is accelerated primarily by the formation of a volatile Si-(OH) phase from reactions between the surface oxides and H₂O vapor. The operating experience thus far with Si₃N₄ turbines is based on unrecuperated cycles, which typically operate at equivalence ratios between 0.6 and 0.8, resulting in H₂O fraction in the exhaust of 6-8% for typical liquid fuels. For the recuperated cycle, the reduced pressure ratio along with a highly effective recuperator minimizes ($T_4 - T_3$) and hence the fuel fraction needed to achieve T_4 . For the proposed engine burning kerosene, the equivalence ratio at full-power with $r = 5.6$ will be 0.18. The benefit is enormous, as **the recession rate is usually quadratic with H₂O partial pressure** [42]. *So recession rate will be reduced by a factor of 15 by reduced equivalence ratio alone.*

**** **Operate at lower pressures and velocities.** Schenk's recent data [3] show a nearly quadratic relationship between total pressure and recession rates over a wide range of pressures (1-20 bar) and velocities (35-500 m/s) for AS800. For AS800, the loss rate increases by a factor of 2.4-3 for each 100 K increase in temperature throughout the 1250-1800 K range, though the temperature dependence is considerably less (a factor of 1.5-2 per 100 K) for most other grades. The loss rate also increases roughly as the 0.6 power of the gas velocity, though there is huge uncertainty here.

Use a high-purity Lutetium-based grade. The oxidation resistance of the lutetium grades is inherently much better than seen in all other grades, perhaps largely because the ultra-low viscosity of the glassy phase dramatically reduces diffusion of oxygen into the base material. Several recent studies have shown that pitting and surface cracks are inversely correlated with the viscosity of glassy phases, especially those formed near the surface by the diffusion of impurities from the bulk material to the surface [17, 43]. Since strain rates near the surface in SN282 are 3 to 4 orders of magnitude smaller than in AS800 above 1650 K, one would expect dramatically lower diffusion and hence a huge advantage in oxidation resistance. Some studies on the oxidation resistance of SN282 were inconclusive, and it seems the explanation is that some early batches of SN282 contained considerable impurities, including Na, Ca, Mg, Yb, and Al [43].

Very recent experiments by two leading groups have shown oxidation/recession rates in high-purity Lu-Si₃N₄ and Lu-Si-Si₃N₄ are lower than seen in Y-Si₃N₄ by a factor of 3 to 8 in dry air at 1500-1800 K [39, 44], and lower than seen in AS800 (La-Y-Si₃N₄) by well over an order of magnitude [39]. The advantage is reported to be considerably greater in moist air [44].

We have begun evaluating a special, high-purity Lu-Si₃N₄ grade with superior mechanical properties. Extrapolations from early data [3, 41, 43, etc.] suggest a recession rate of ~0.1 mm in 10,000 hr for an equivalence ratio of 0.25 at 550 kPa and 1600 K. This is also roughly in agreement with extrapolations from recent data by Klemm [39] and Asayama [44]. **We plan to evaluate the oxidation resistance of several silicon nitrides, including a high-purity Lu-Si₃N₄, in various exhaust atmospheres to at least 1400 K during the Phase I.**

**** **Optimize the geometry to minimize flow velocities very near the surface at the edges.** While densities and temperatures are lowest at the trailing edge of the blade, this edge is generally more than an order of magnitude sharper than the leading edge of the blade. As a result, relative velocities 2 microns from the surface can be an order or magnitude higher than at the leading edge. This partially explains the observation that recession from the trailing edge is higher than at the leading edge [45]. Our preliminary simulations showed that novel blade geometries can reduce the maximum relative velocities 2 microns from the surface near the leading and trailing edges by factors of 3-6 (to relative Mach # 's below 0.1) with minimal loss in efficiency when

properly optimized. It appears that the final ε penalty will be $<1\%$ for a substantial increase in lifetime. (See **Figure 8** for a very preliminary radial-flow Si_3N_4 turbine.)

**** **Summary of recession minimization in Si_3N_4 .** At this point, in stark contrast to widely accepted beliefs throughout the industry, we feel the investigation and development of coatings for ceramic turbines need not be a high priority. We expect that with high-purity Lu- Si_3N_4 in a highly recuperated cycle with properly designed uncoated turbines, lifetimes in excess of 20,000 hours will be obtained for: (a) 15 kW engines up to 1520 K TIT, (b) 100 kW engines up to 1620 K, and (c) 1000 kW engines up to 1720 K. Moreover, it is reasonable to plan on a 10,000-20,000 hour replacement schedule for the first-stage turbine and stator. If longer life is desired, it appears that a reaction-bonded $\text{Lu}_2\text{Si}_2\text{O}_7$ coating can further improve oxidation resistance [44].

**** **3.2.4 The Turbine Design.** Undoubtedly, the single most important lesson learned from the AlliedSignal Ceramic Gas Turbine Technology Development program (which had substantial DOE, NASA, DoD, and DARPA support) during the 90's was that the approach that had been standard practice with axial-flow metal turbines – mounting individual turbine blades in a disk – was impracticable with ceramics. The only possible approach is a monolithic blisk [3]. Unfortunately, they may have not fully comprehended the implications of the second most important lesson: that ceramics have much lower impact strength and vibration tolerance than metals and thus are ill-suited to axial-flow turbines.

**** **3.2.4.1 Solving the FOD Problem.** The best approach is to use monolithic radial-flow turbines (in which the blades can have order-of-magnitude higher impact strength and blade resonant frequencies than in axial-flow turbines) and solve the Foreign Object Damage (FOD) problem by (1) eliminating the regenerator, (2) preventing carbon deposition and subsequent spalling, (3) improving oxidation and creep resistance of Si_3N_4 , and (4) preventing ingestion of damaging particles. The last two items were a focus of the Japanese Automotive Ceramic Gas Turbine Program [2], which is probably the closest prior work to our general design, though there are a number of major advantages in our approach, as noted earlier in section 1.3, Table 2, and more specifically on page 8. We do not expect FOD to be a serious issue in our engine for the following reasons:

*** 1. After ceramic regenerators (which are notoriously friable), the primary source of foreign objects is spalled carbon from the fuel vaporizer or combustor. Using an alumina boiling surface at 400-450°C has been shown to eliminate carbon deposition in the vaporizer, even with moderate-grade fuels [15, 46]; and the CFD simulations of our vapor-fed micro-jet ultra-lean combustor show no carbon or UBC generation there.

*** 2. From what has recently been learned about the accelerating creep rates in the surface layers of some silicon nitrides subjected to oxidizing exhaust streams, it seems likely that many failures have actually been due to creep-enhanced sub-critical crack growth in these materials. The creep rates in the surface layer of Lu- Si_3N_4 are lower by over three orders of magnitude than in the most commonly used earlier grade, AS800, so this weakening mechanism is not likely to be significant in our turbine material.

*** 3. Blade thickness near the root near mid-chord in a radial flow turbine can be increased by a factor of four compared to standard practice in metal turbines with very little loss in aerodynamic efficiency if appropriate compensating changes are made (in number of blades, entrance and exit angles, twist, hub and shroud profiles, etc.) [47]. This permits greatly enhanced resistance to FOD, as the kinetic energy for fracture is approximately proportional to the square of the product of fracture toughness (which is usually measured only at RT) and mid-blade thickness [48]. (This correlation is much better than a Weibull modulus correlation [48].)

**** Turbine optimization requires simultaneous consideration of at least five tightly coupled, complex problems: (1) aerodynamic (with CHT) optimization, (2) blade stress minimization, (3) maximizing impact strength, (4) erosion minimization/accommodation, and (5) manufacturability. A preliminary, starting point for the first-stage turbine design is shown in **Figure 8**. Separate soft-

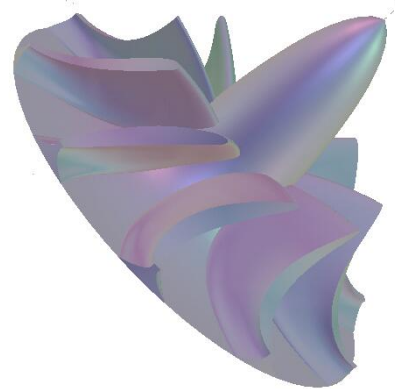


**** Figure 8. A very preliminary Si_3N_4 turbine design. The tip OD is ~ 72 mm.

ware and methods are required to address each of these problems, making true optimization quite complex. Our experience in producing efficient radial-flow Si_3N_4 micro-turbines (albeit for a much lower flow regime) gives us a unique perspective on this complex problem; and the blade geometry modification software we have developed nicely complements our advanced commercial software (Numeca FINE/Turbo 5.3, Fluent 6.0, and CFX-BladeGenPlus 4.1) for accurate evaluation and optimization of novel blade geometries using genetic-based algorithms and neural-networked databases.

**** At this point, it appears the tip speed will need to increase to ~600 m/s at 1800 K TIT, which will result in ~200 MPa peak stress for current designs. For SN282, this is compatible with 10,000 hour rupture life in small parts; however, it appears likely that genetic-algorithm-based optimizations will permit substantial reduction in peak stress (with negligible loss in efficiency) for greatly increased lifetime and robustness, even with Weibull modulus only ~12. Moreover, there is very recent preliminary data suggesting that Lu-Si- Si_3N_4 grades may achieve 600 MPa short-term rupture strength at 1770 K and Weibull modulus up to 20 [44], though this data has been questioned by a competitor [45]. For TIT up to 1570 K, a superalloy can be used for the second stage nozzles. With 1400 K TIT in our initial engine, an MA superalloy will also be suitable for the first stage nozzles.

3.2.4.2 Optimization using Genetic-based Algorithms. We recently completed a comparative evaluation of two advanced CFD codes known to be particularly well suited for turbomachinery – CFX TaskFlow and a more recent contender, Numeca FINE/Turbo. Both solvers are based on Reynolds-stress-averaged Navier Stokes (RANS) equations (the coupled energy, mass, and momentum conservation equations) on structured grids, but TASCFlow uses pressure-based pre-conditioning and algebraic multigriding while Numeca uses density-based pre-conditioning and geometric multigriding. Also, Numeca offers a wider variety of more-advanced turbulence models to choose from. We found FINE/Turbo to agree with the validation experiments we performed on micro-nozzles within our experimental error of ~2% over a wide range of conditions, while TASCFlow errors were somewhat greater. We also found the Numeca tools to be much more convenient (after an acceptable learning curve) for turbine blade optimization and computationally more efficient by at least 40%, as judged by the time required to reach acceptable convergence on the same platform. Most likely, the improved computational efficiency is partially due to the better quality meshes (especially, the improved clustering) generated by Numeca's Autogrid compared to AEA's Turbogrid.

We were also impressed with the progress Numeca has made in fully automating the system optimization problem mentioned earlier of integrating CFD, FEA, cost, and lifetime constraints through the use of a neural network managing a custom database of CFD results within the design space established by the genetic-based optimization algorithm in FINE/Design3D [49]. (It is worth noting that neither AEA-CFX nor Fluent have plans to do anything similar.) This software is still in the beta phase, but a number of validations have shown it to be promising. The primary task is to devise a suitable objective function that properly weights all of the important parameters: efficiency, pressure ratio, peak stress, rms stress, outlet flow angle, isentropic Mach number distribution on the blade surfaces, impact strength, edge radii, lifetime, and manufacturing cost. In some cases, suitable functions must be developed to determine these parameters from available variables and parameters.

A database of results from 50-100 CFD calculations over the allowable parameter space is calculated to produce the first generation. Then pairs of individuals (calculations) are selected from this population based on their objective function values. The performance of an individual is denoted its "fitness". Then each pair of individuals undergoes a reproduction mechanism to generate a new population in such a way that fitter individuals spread their genes with higher probability. The

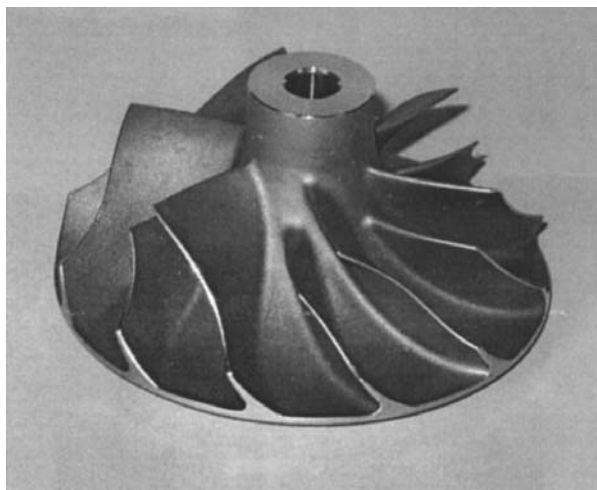


Figure 9. The Garrett T3, trim 60, turbo-charger impeller is shown here. The tip OD is 60 mm.

children replace their parents. As this proceeds, inferior traits in the pool die out and strong traits tend to combine to produce children who perform better. A particular strength of the genetic algorithm is that it does not tend to get trapped in local minima.

3.3 The Compressor. As noted earlier, two-stage compression with intercool will be used for higher system efficiency, reduced system mass (because of the increase in optimum r), extended off-design performance, and reduced acoustic noise. The benefit of 2-stage compression in acoustic noise reduction is quite significant. The recuperator almost completely muffles (25-30 dB attenuation) the outlet noise from the compressor and both the inlet and outlet noise from the expander. The outlet noise from the first stage compressor and inlet noise from the second stage is silenced by the intercooler. The primary remaining acoustic source is the inlet noise from the first stage compressor, which is reduced because of the low stage-pressure ratio and is minimized by using a vaneless diffuser for the first stage [50].

To keep the cost down during the early phases of the development and demonstration, we will use off-the-shelf turbocharger compressor impellers, as shown in **Figure 9**. Well designed turbocharger impellers, optimized for mass flow from 0.08 to 0.3 kg/s are readily available at retail prices of \$77-180 each [51]. Smaller turbocharger impellers are available on special-order from IHI Turbo America, formerly IHI-Warner [52]. After the initial demonstrations with off-the-shelf turbocharger impellers, compressor impellers more specifically optimized for the design conditions (with increased sweep back, extended vaneless diffuser, etc. [53]) will be developed using the genetic-based Numeca FINE/Design3D.

The Garrett T3, trim 50 (\$77), is likely to be selected as the first-stage compressor impeller. A performance map when used in a standard turbocharger housing is shown in **Figure 10**. With tighter control over tip clearance and a larger vaneless diffuser, the CFD simulations indicate efficiency should be 5-8% better. The IHI RHF3 is likely to be selected for the second-stage impeller. For optimal control, both modified compressors will require considerable detailed CFD for accurate maps over the full range of operating conditions.

There has been considerable success recently in surge control using a close-coupled valve, a regulated exit plenum, condition sensors, and a fast-response high-gain control algorithm [54]. The effect is to eliminate the flow oscillations that otherwise lead to surge or rotating stall on the low-flow side of the high-performance island. This has allowed safe operation at higher efficiency over a wide range of off-design conditions. However, we expect to keep the turbomachinery conditions highly optimal using other available control mechanisms, as discussed later (see section 3.9) in more detail.

3.4 The Spindle Bearings. For more than a decade, we have found our supersonic gas bearings to be indispensable in our high-speed micro-turbine-driven NMR sample spinners [30, 31] and in our reverse Brayton cycle (RBC) cryocooler developments [13]. We also note that gas-bearings are currently used in some commercial 25-50 kW microturbines [7] and are highly regarded by some researchers [55], so a few comments are in order before turning to the current choice, oil-lubricated Si_3N_4 ball bearings.

Gas bearings have very low stiffness, which has very detrimental implications in variable speed microturbines and makes operation at high altitudes impossible. Also, our experience with a very wide range of gas-bearing-supported micro-turbine-driven rotors over the past two decades

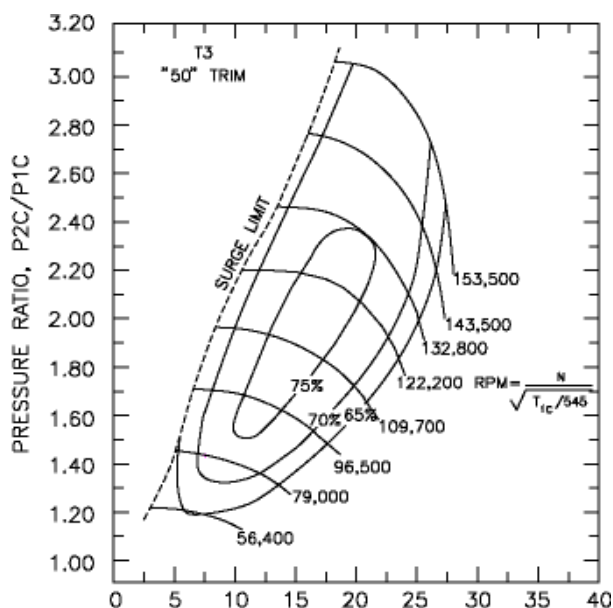


Figure 10. Manufacturer's performance map of polytropic efficiency contours for the Garrett T3 Trim 50 (slightly smaller inducer than the Trim 60 of Fig. 9) in a standard turbocharger. Horizontal axis is lb/min at STP.

has consistently found it extremely difficult to maintain stability at rates much above twice the fundamental conical resonance mode of the spindle, even with our effective whirl-suppression schemes [56]. This sets a lower limit on the ratio of the bearing stiffness to the spindle's transverse moment of inertia [30]. Adequate radial stiffness k_r is obtained only with relatively large surface area. For the hydrostatic gas bearing at sea level,

$$k_r \cong A(\rho_1 - \rho_0)/\pi r_c \quad [8]$$

where A is the bearing surface area (m^2), ρ_1 is the inlet pressure (Pa), ρ_0 is the outlet pressure, and r_c is the radial clearance (m). For the dynamic (e.g., foil-backed) gas bearing, the effective $(\rho_1 - \rho_0)$ is velocity dependent. The clearance r_c is also velocity dependent and typically 5-20% of that found in a hydrostatic bearing under similar load. However, the compliance of the foil support (needed for stability and to accommodate changes in r_c) appears in series with that of the air-film and hence reduces the total bearing stiffness substantially [57]. As a result, typical radial stiffness in bearings similar to those used in current 30 kW (Capstone) MGTs with air bearings (35 mm diameter) is only $\sim 3.5 \times 10^5$ N/m (for each end). The first mode is $\sim 10,000$ rpm, and eccentricity approaches unity [57].

The frictional power loss P_f of an *ideal* gas bearing (assuming no Taylor vortices and neglecting the pumping power needed for the hydrostatic bearing) is approximately

$$P_f \cong \mu v^2 A/r_c \propto \mu v^2 k_r \quad [9]$$

where μ is the dynamic viscosity of the gas (1.8×10^{-5} kg/m/s for air at 300 K) and v is the bearing surface velocity (m/s). Our experimental data show that Taylor vortices cause losses to be 3-5 times higher than the above simplistic estimate, depending primarily on vr_c [30, 58]. For the dynamic bearing, the bearing friction is 2-4 times higher yet (primarily because mean r_c is reduced by a factor of 3-10). Since the radial gas bearing has essentially zero axial stiffness, separate axial thrust bearings are required.

**** **Frictional power loss for the 30 kW Capstone radial air bearings alone at 100,000 rpm is at least 400 W [57].** The large shaft diameter and the necessarily short overhang distance to the turbine (because of the poor stiffness of gas bearings) result in a lot of heat conduction into the bearing shaft and on into the aluminum compressor impeller. This conjugate heat transfer degrades the compressor efficiency by $\sim 3\%$ and turbine efficiency by $\sim 2\%$. The excessive (axial) tip clearance required by the poor axial stiffness further degrades both ϕ and ε by another 2-4% each. This probably explains why Capstone gets only 79% polytropic efficiency in their compressor and 83% in their expander at $r=3.9$, 0.5 kg/s, 50 kW [6]. **Hence, much of the poor efficiency of current MGTs below 60 kW seems attributable to the use of air bearings.**

Ceramic ball-bearing technology, on the other hand, has made enormous progress in the past four years because of silicon-nitride, though published data on frictional power loss in silicon nitride composite ball bearings are inconsistent and vague [59]. Hence, we recently designed and constructed a ball bearing test apparatus to permit accurate friction measurements on ball bearings of 12.7 mm ID at up to $\sim 150,000$ rpm.

**** Our recent experiments show the frictional loss of an oil-lubricated 12.7 mm Si_3N_4 composite ball bearing at 140,000 rpm **is only ~ 50 W**. Moreover, compared to Capstone's air bearings, its radial stiffness is ~ 400 times greater, and its axial stiffness advantage is even greater yet.

The requirement of sufficient axial distance between the hot expander and the ball bearings for adequate bearing and seal cooling with sufficient shaft stiffness can easily be met with a 12 mm shaft. The tapered, oil-lubricated, 12 mm spindle bearings have an expected lifetime of 20,000 hours at 125,000 rpm – the expected design speed in the proposed 30 kW turbo-generator. For high radial stiffness, adjustable axial loading and shimming are required. Precise axial positioning of the two turbines and two impellers relative to their respective shrouds is handled most easily with separable spindles, each with two bearings. The parts cost for replacing the eight bearings will be $\sim \$500$, and the labor cost should be comparable.

3.5 The Spindle Designs. Like ceramic turbine design optimization, MGT spindle design optimization is a complex and iterative process involving some disparate objectives that do not appear to have been fully appreciated by most prior MGT groups. The following requirements must be optimally balanced:

1. Minimization and accommodation of thermal stresses, strains, and distortion;

2. Compatibility with precision and reliable attachment of a Si_3N_4 turbine to a metallic shaft;
3. Minimization of hot corrosion – especially where it affects tip or hub leakage;
4. Compatibility with simplified spindle manufacturing, assembly, and service;
5. Elimination of weakly damped vibrational modes throughout the full operating range;
6. Minimization of cost of materials (i.e., volume of ceramic stator);
7. Delivery of inlet flow to the turbine uniformly at the required magnitude and direction vectors;
8. Minimization of losses from turbulence leading into and around the scroll;
9. Minimization of tip-gap clearance throughout the normal range of operating conditions;
10. Minimization of heat transfer (from all sources) into the compressor impeller;
11. Minimization of heat leak from the turbine – especially into the bearings;
12. Maintenance of required bearing and oil-seal temperatures (at least if oil lubricated);
13. Minimization of turbine-hub-flow (back-side) leakage, and minimization of windage losses;
14. Lubrication of the bearings.

**** The first six items listed above have each appeared (indirectly) near the top of one or more lists of "lessons learned" or discussions found at the end of previous (unsuccessful) ceramic gas turbine efforts [2, 3, 15, 16]. Perhaps the most serious mistake would be to develop an emotional attachment to a design that may have some aesthetic appeal, apparent patent protection, or useful legacy, but fails to consider all of the above points (as, for example, appears to be the case with Capstone, Honeywell, Ingersoll-Rand, etc.). Most prior MGT designs above 50 kW (except, most notably, Capstone) have used two-stage expansion, with one stage (the "gasifier") driving the compressor and the other stage driving the gear box to the load.

Our analysis indicates most of the above objectives are best satisfied in a 2-stage design using four separable spindles. Only windage is greatly worsened, but it is by far the least significant concern. Bearing cost is increased, but this is a small price to pay for greatly simplified assembly and service, reduced thermal stresses, improved compatibility with joining ceramic stators to metallic bearing housings and ceramic turbines to metallic shafts, minimal use of expensive ceramics, improved tip-gap control, and reduced impeller heating.

**** A cross-section of a very preliminary 1st-stage expander spindle design is illustrated in **Figure 11** and helps to clarify some of the major differences between our proposed approach for a 30 kW MGT and traditional designs that have been used with superalloy radial turbines in the 25-150 kW range. Some of the differences stem from the difficulty of mounting a Si_3N_4 turbine on an overhung superalloy shaft in a way that (1) permits simple assembly and disassembly, (2) is compatible with the differential expansion between Si_3N_4 and superalloys [60], (3) keeps the critical modes well away from the operating range, and (4) keeps the bearing oil-seal temperature below $\sim 80^\circ\text{C}$. A gas seal on the shaft keeps hub leakage extremely low without

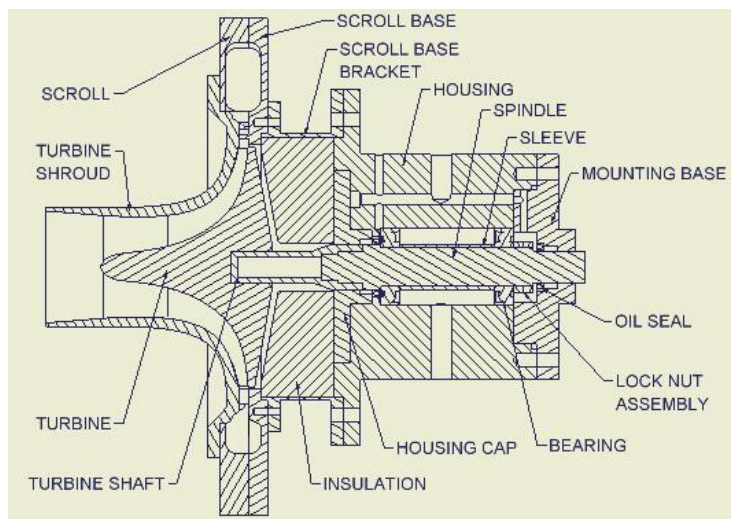


**** Figure 11. Very preliminary expander spindle design.

needing tight clearance on the back side of the turbine. Turbine tip clearance is easily controlled with little concern about shaft expansion beyond the first bearing. It appears the 1st-stage turbine may be supported on a hollow superalloy shaft for TIT up to ~ 1670 K using MA-6000. And again, we emphasize that the spindles are expected to be an order of magnitude easier to assemble and disassemble than most previous designs (i.e., those of Capstone, the Japanese ceramic MGTs, etc), though the details supporting this claim are not all apparent in Figure 11.

Considerable progress has been made recently in ceramic-to-metal joining technology. We have obtained brazement strengths of 250 MPa to Si_3N_4 with a vacuum brazing process using a Ag-Cu-Ti alloy [61], and a similar technique has reportedly achieved silicon-nitride brazement rupture strengths approaching 600 MPa [62]. Higher temperature active brazes based on Ti-V-Cr

with 1800 K solidus have had some success [63]. However, the real challenge with high-temperature brazes to silicon nitride is the enormous stress that develops from the differential thermal expansion during thermal cycling. Kyocera claims to have proprietary processes that are effective for high-temperature joints, but details are not available.

**** We have recently demonstrated successful diffusion bonding between silicon-nitride components in microturbine sample spinners that are currently in production. The joints appear reliable with thermal cycling to at least 1730 K, which is 160 K beyond what is expected to be required for 1800 K TIT. We plan to evaluate a novel related process that we expect to be reliable for the required Si₃N₄-to-metal shaft bonding in the expander spindles. Our analysis, based on considerable experience with high-temperature ceramic joining, gives us reason to believe that we will not experience problems in this joint with repeated thermal cycling.

**** We find it most convenient to analyze the spindle heat-flow/cooling problem using an electrical circuit analogy and standard, linear-circuit-analysis software. The heat-flow problem in the expander spindle assembly can be adequately approximated by a simple network containing ~16 lumped thermal resistors, 10 nodes, and four fixed voltages corresponding to known boundary temperatures. In the thermal simulation, the nozzles are at 1400 K (the TIT), the turbine inlet tip is 1200 K (the relative or rotating-frame total temperature is appropriate here), and the exducer blades are at 1180 K. While the total heat leak from the fibrous-zirconia-insulated scroll may be ~500 W, the heat conduction down the thin-walled turbine-support shaft into the bearings can be kept low enough for the oil seal and first bearing to easily stay below ~350 K.

**** The bending mode frequencies for a uniform spindle on two ball bearings of infinite radial stiffness are easily calculated using published equations for various conditions, including closely spaced bearings with extreme overhang [64]. We used a perturbation modification of the latter conditions for a quick estimate of the first and second modes for the complex geometry of the proposed spindle. The first mode is estimated to be ~800 Hz, and the second mode ~6 kHz. The lowest operating rotational rate will be ~900 Hz and the highest ~2200 Hz, so smooth response over the operating range is expected. **A more detailed analysis will be performed during Phase I to more accurately predict the critical frequencies, which can easily be adjusted if needed.**

**** Spring-loaded, graphite-reinforced-Teflon oil-seals are available with p_v ratings up to 430,000 psi-fpm (15 MPa-m/s). The spindle is designed so that these seals can easily be replaced at regular intervals – perhaps every 2000 hours if necessary. There may be difficulty in obtaining long lifetime from these oil seals at the anticipated surface speeds of ~80 m/s, even at minimal seal pressures. Teflon-graphite-filled polyimides (e.g., vespel SP-211) are available with lower wear rates and lower friction coefficients for air service at higher p_v factors, though wear data are not available for oil service at extreme conditions. **Fabrication and testing of custom oil seals from vespel SP-211 at surface speeds above 80 m/s with several lubricants is needed to ascertain lifetime under anticipated engine conditions.** Not all of the details are apparent in the cross-section of Figure 10, but **these points will be well addressed and all parts fully detailed for the first-stage expander spindle in the advanced 3D CAD tool "Inventor" during the Phase I.** Of course, four spindles are required, and preliminary design work will also be completed on second-stage expander and the two compressor spindles, which are simple by comparison.

3.6 Low-emissions, High-stability Combustion Using Micro-jets.

It is well known that negligible thermal-origin NO_x is generated if peak combustion temperatures stay below 1700 K in mid-sized combustors [14]. Hence, the standard approach to limiting peak combustion temperatures in the unrecuperated cycle is some form of lean premix, though this is inherently unstable. The primary challenge is achieving stability as the equivalence ratio decreases, as high turbulence increases the tendency of flame extinction near the lean limit at low air-inlet temperature T_3 and it increases the tendency for flashback at high pressure and high T_3 . Obtaining stability over a reasonable range of temperatures, pressures, and very lean equivalence ratios without the use of catalysts has been extremely challenging [2]. However, catalysts have complex start-up and staging issues, add considerable mass and cost to the combustor, and have limited lifetime for TIT above ~1250 K [65]. One measure that can be taken to improve stability at high T_3 and reduce NO_x is to inject a fully vaporized fuel [14]. But for T_3 beyond ~930 K, the autoignition delay is too short to control in a lean-premixed flame over a

reasonable range of conditions [2]. Fortunately, small, single-phase flames are much more amenable to CFD methods than are combustors with atomized droplets and intense, large-scale turbulence [66], so one can explore novel, small combustor designs with reasonable confidence. In collaboration with Prof. Jamil Khan at U.S.C., we investigated several configurations for micro-jet gaseous-fuel autoignition combustors using Fluent 6.0.

A diffusion flame is inherently stable over an extremely broad range of lean exit equivalence ratios; and for T_3 above the autoignition temperature at the flow-residence time, there is no flameout lean-limit. However, one must limit the peak combustion temperature that occurs in the stoichiometric boundary between the rich and lean zones and/or dramatically reduce the time at the peak temperatures. Because of the 2/3-power relation between surface area and volume, micro diffusion flames see peak temperatures that are somewhat reduced by radiation, conduction, and convection, and residence times are extremely short. We looked at combining a large number of micro diffusion flames but found it impractical to achieve low NO_x for combustor power above a few kilowatts with this approach for the required conditions. The lowest NO_x we achieved with this approach in a combustor suitable for a 10 kW engine with $\text{TIT}=1400$ K was over 300 ppm, which we mention only as a reference point for what follows.

**** The best approach seems to be a novel method we call *rapid lean micro mix*. Since there is no flameout lean-limit for high T_3 , we can achieve the desired objectives by injecting the fully vaporized fuel at high velocity transversely into the path of hot air jets to achieve ultra rapid mixing and dilution. In our method, the vaporized fuel (at ~ 750 K) is injected from several well-spaced jets, each under 0.6 mm diameter, at relatively high velocities (mach # ~ 0.2) near the perimeter of the base of the combustor can. Most of the air (at ~ 950 K) is injected with high swirl through several circles of small holes (of under 5 mm diameter) on the cylindrical surface very near the base at mach number up to 0.16. *The transition through stoichiometry occurs in tens of micro-seconds over just a few millimeters in the jet-intersection zones while the mixture is relatively cool.*

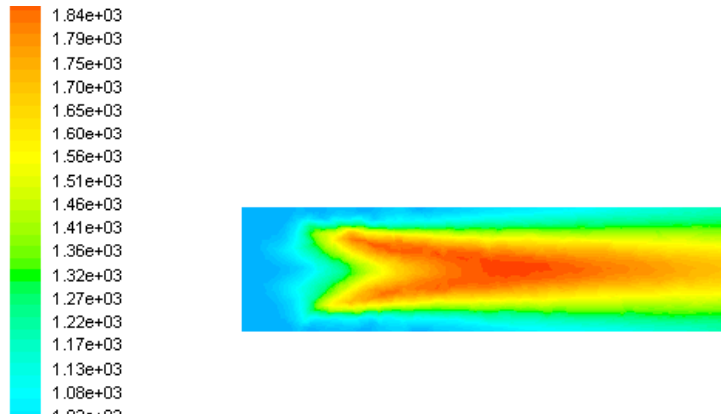


**** Figure 12. Central-plane temperature plot in an autoignition micro-jet combustor of 6 cm diameter. (We note that the outlet pattern factor is of no real concern, as it may be addressed by standard methods.)

**** Unlike lean pre-mix, in which one relies on a relatively large mixing/dilution zone prior to combustion and a flame holder to help define the combustion zone, in rapid-lean-micro-mix, combustion begins immediately (though relatively slowly initially) at the point of fuel injection and accelerates rapidly for several tenths of a millisecond. But peak temperatures are limited, as $\sim 50\%$ of the mixing/dilution is achieved within ~ 0.3 ms of fuel injection. The dilute mixture is achieved so rapidly that so significant combustion occurs under near-stoichiometric conditions.

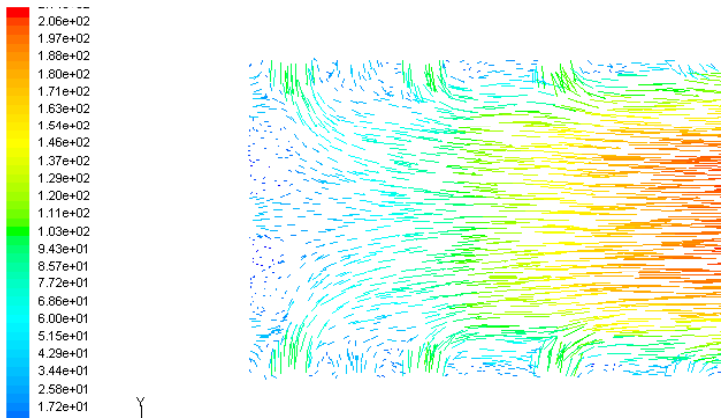


**** Figure 13. Central-plane velocity plot for the inlet portion of the combustor of Figure 12. The mean outlet Mach number is ~ 0.2

**** A moderate-flow-rate case (0.043 kg/s air, appropriate for a 10 kW engine) with vaporized kerosene fuel gave peak temperature ~ 1930 K, residence time in the hot zone ~ 0.3 ms and mean exit NO_x below 0.02 ppm. The temperature and velocity

profiles are shown in **Figures 12 and 13** respectively. For a mean exit temperature of ~ 1380 K, both vaporized octane (C_8H_{18}) and kerosene gave **NO_x well below 0.1 ppm over a wide range of conditions**. At much lower flow rates, the hot-zone-residence time may increase by an order of magnitude but the peak temperature will drop ~ 200 K, so NO_x still drops. There is, however, significant CO production in the combustion chamber; but that is not a concern, as it will be fully oxidized before it exhausts a third of the way through the recuperator. (The reaction rates for oxidation of CO and UBC at 950-1100 K are very fast compared to the 10 ms residence time in this portion of the recuperator.) There will also be some reduction of the NO_x in the recuperator, assisted by catalytic reactions at the surfaces of the superalloys. **We will begin looking at this during the Phase I.**

Of course, there is considerable uncertainty in these results, as Fluent 6.0, though generally recognized as the most validated combustion code available, has probably not been well validated in the autoignition ultra-lean regimes seen in our combustor. Also, we used only $\sim 112K$ tetrahedral cells with limited mesh refinement. Some of the next steps include further mesh refinement in the high-gradient zones, the use of hexahedral cells, and comparisons to other codes, – especially the new flamelet combustion code in soon-to-be-released AEA CFX 5.6. And of course, we need to look at the combustor over the full range of operating conditions. **This work will be carried out during the Phase I.** Also, we will look at several common fuels, including kerosene, methane, ethanol, H_2 , and JP-8 (which can be adequately modeled as 34.7% n- $C_{12}H_{26}$ (dodecane), 32.6% n- $C_{10}H_{22}$ (decane), 16% $C_{10}H_{14}$ (butylbenzene), and 16.7% a- C_7H_{14} (methylcyclohexane) [67]).

3.7 Compact Ultra-high-temperature Recuperators. Cross-corrugated (CC) recuperators [28] currently in production (with straightforward modifications in their ducts and manifolding) will be fully suitable for demonstration purposes of the second-generation MGT as proposed herein: 1400 K TIT, intercooled compression, Si_3N_4 first-stage turbine, superalloy second-stage turbine, etc. The increase in turbine outlet temperature T_5 from 910 K (current MGTs) to 1070 K will shorten recuperator lifetime for the current standard material (SS447) by nearly two orders of magnitude, but much longer lifetime can be achieved by simply changing to a ductile superalloy. A recent study evaluated a number of candidate alloys largely on the basis of creep-rupture life at 100 MPa at $750^\circ C$ [68, 69]. The two most significant problems with this study were that (1) average stresses in CC recuperators are closer to 30 MPa and even peak stresses of 100 MPa are not present for very long periods (as the material creeps/deforms in such a way as to reduce the peak stresses) and (2) corrosion in the exhaust environment at elevated temperatures is often a more severe factor than creep rupture in determining lifetime. As a result of the unrealistically high stress in the above study, the materials always failed relatively quickly. Still, the conclusion that Haynes alloy HR-120 (37Ni, 33Fe, 25Cr, 2Mo, 1.5W, 0.7Nb) may be the preferred alloy for second-generation CC recuperators seems valid, as it represents an excellent balance between performance and material cost – which is about three times that of SS347. While the data do not permit accurate estimates of lifetime, a reasonable estimate is $\sim 10,000$ hours.

Because of the large investment that will be required to develop the manufacturing process for a novel, low-stress, ultra-compact, high-effectiveness, high-temperature recuperator, it seems premature to put substantial resources into such a program at this point in time. It is much more cost-effective to use existing CC recuperator technology with the relatively simple change from SS347 to HR-120 for 2nd generation MGTs.

It is important, however, to appreciate that, while a CC recuperator made of HR-120 could be used for short-term experiments at even higher temperatures, a simple solution does not exist for long-life recuperators for 3rd-generation MGTs, where T_5 goes to 1160 K and r increases to 6.8. Indeed, better superalloys are available; but, irrespective of the cost, those that are compatible with the manufacturing process simply will not offer lifetimes above ~ 1000 hours for these conditions. Of course, it is possible that the current intensive work on fuel cells, where ultra-compact high-temperature recuperators are also often needed [9], will produce a suitable recuperator; but this seems unlikely, as many requirements (especially, relative flow rates and coking and oxidation resistance) are quite different. Hence, it is important to have a well-thought-out plan for novel, long-life MGT recuperators beyond 2nd generation.

The huge efficiency advantage of a 500-650 K increase in TIT cannot be realized without recuperators designed to (1) be compatible with large-scale manufacturing from a readily

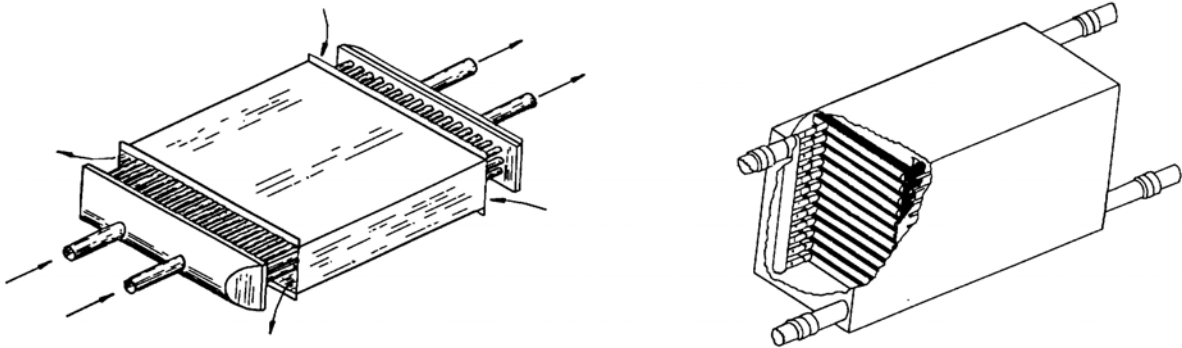
weldable, ductile *superalloy* of very high hot-corrosion resistance and creep strength, (2) minimize thermal stress, (3) eliminate highly stressed elements, and (4) minimize superalloy utilization.

It is generally accepted that brazed-plate or stamped, folded-foil designs have inherent advantages as compact heat exchangers. There is no denying that brazed-plate exchangers are currently the most cost-effective commercially available solution for compact recuperator applications. But there are sound engineering reasons, well presented many times in the past [18, 27, 70], why plate-type exchangers cannot be ideal for a very-high-temperature recuperator, partially because peak stresses in the brazed-plate designs are an order of magnitude higher than in microtube designs. Another very important advantage of our Micro-Tube-Strip (**MTS**) design is its ability to achieve reduced pressure-drops compared to compact, turbulent-flow recuperators.

Utrianinen and Sunden have calculated the theoretical core mass and core pressure drop for a number of published compact designs [28], but the bottom line is better summarized by first looking at the mass and performance of the final product. More precisely, we quantify compactness by specific conductance, **SC**, heat transfer power per degree of temperature difference T_δ between the counterflowing streams, W/kgK. (We include recuperator manifolding but not external insulation in the mass for the SC calculation.) Then, one must look at pressure-drop on the low-pressure side (the pressure drop on the high-pressure side is generally insignificant) and the material and joint stresses, as these determine the upper temperature limit.

A recent MGT (from Capstone) uses a folded-foil recuperator with 87% effectiveness, total normalized pressure drop of 10%, with $SC \cong 28$ W/kgK. This translates into a Recuperator Specific Mass **RSM** of about 2.1 kg/kW_E (recuperator mass, not including ducts and insulation, per kW of P_E) for the Capstone MGT with T_5 of 910 K.

We have recently demonstrated 800-tube MTS modules using CuNi microtubes of $d_o = 0.8$ mm (OD) and $d_i = 0.64$ mm (ID). Such an exchanger from superalloy microtubing would be capable of 92% effectiveness with specific conductance ~ 150 W/kgK (five times that of the Capstone unit) and total pressure drop $\sim 13\%$. Of course there are several caveats. First, the above exchanger was a hand-assembled prototype. Second, the materials used in the above experiment (CuNi tubing and Ag braze alloys) were not suitable for high-temperature use. Third, it would be rather expensive to produce. However, our analysis suggests a design utilizing microtubes of 1.27 mm OD, 1.07 mm ID, and 0.7 m length could have competitive manufacturing costs, an SC of 75 W/kgK, and pressure drop of $\sim 5\%$ at 92% effectiveness for low-altitude applications. Most importantly, it could be compatible with long lifetime for T_5 up to 1300 K because it minimizes both thermal and pressure-dependent stresses. **Peak material stress in MTS recuperators in 4th-generation MGTs, where $r = 7.2$, would be only 4.4 MPa.**



Figures 14a, 14b. MTS exchanger module concept, and bank of 12 parallel MTS modules.

The design is conceptually simple, as illustrated crudely in **Figures 14a and 14b**. A key realization here is that in compact, high η_x recuperators, where flows are predominately laminar, SC is relatively independent of both pressures and flow rates, and it is roughly proportional to d_o^{-2} [18, 21, 27]. Moreover, for high-effectiveness laminar exchangers, the minimum tube ID d_{min} is quite small and is given approximately by the following:

$$d_{min} \cong 1000 (k\mu T_\delta)^{1/2} / [(T_H - T_C)\rho C_P] \quad [10]$$

where k is the gas conductivity (W/mK), μ is the dynamic viscosity (kg/ms), ρ is the gas density (kg/m^3), T_H is the highest temperature, T_C is the lowest temperature, and C_p is gas specific heat. This amounts to ~ 0.5 mm for the typical recuperator at sea level, and ~ 1.4 mm at 10 km altitude.

**** Micro-tubing can be produced from easily weldable, ductile, metals, including superalloys, at very low cost; so essentially the object is to devise an effective method of manifolding thousands of parallel microtubes such that highly uniform counterflow conditions are achieved over most (preferably at least 90%) of the length of the tubes and thermal stresses are minimized. For the sake of brevity, we do not present analysis and design here in detail. For the 3rd or 4th-generation MGT, the optimum module is expected to comprise 10 rows of 80 tubes per row. Each microtube is expected to have 1.27 mm OD, 1.07 mm ID, and 0.7 m length. Seven such modules would be paralleled for a 30 kW MGT. The total volume of such a recuperator, including the external insulation, will be ~ 110 liters, and the total mass (with ducts and insulation) will be ~ 28 kg.

**** Because of the much lower stress and higher temperature in the MTS design compared to plate designs, the alloys being studied in other research programs [69] for advanced recuperator materials are less optimum here. A highly ductile and weldable superalloy is required, and strength is less important than hot-corrosion resistance. For T_5 between 1030 K and 1130 K (2nd generation MGT), the preferred alloy is probably SS-317L because of its much better corrosion resistance than SS-347. (SS317L is very similar to 316 except for slightly higher Ni, Cr, and Mo, with lower C [71]. The 10% lower 100,000-hr rupture strength of 317 at 1070 K is still much more than adequate for MTS recuperator requirements.) For maximum T_5 between 1130 K and 1200 K (3rd generation MGT), the preferred alloy is probably HR-120. For 4th and 5th generation, the preferred alloy appears to be Haynes-230 (55Ni-22Cr-14W-3Co-2Mo-.4Si-.02La). At 1250 K, it has an order of magnitude better hot-corrosion resistance and time to rupture at 5 MPa (100,000 hr) than Inconel 600 (76Ni-15.5Cr-8Fe), and it is two orders of magnitude better than SS-347 [72]. The efficient use of materials and simple design of the MTS exchanger is required for the use of ductile superalloys such as H-230 (which is six times as expensive as SS-347). The exceptional hot corrosion resistance of H-230, along with the low-velocity, laminar flow, and clean-fuel conditions, should permit an 11-year lifetime even for 1800 K TIT ($T_5 = 1300$ K).

**** Fouling has not been a serious problem in cross-corrugated MGT recuperators and is not expected to be a problem in MTS recuperators, as the exhaust-side effective hydraulic diameters are comparable. Moreover, by fabricating the entire recuperator from a corrosion-resistant superalloy, most deposits could be burned out by reversing the flow periodically. (Of course, exhaust would always be shellside.) Deposits that resist burnout could be removed by acid cleaning – perhaps every five years.

**** It should also be noted that the engine's thermal time constant (warm-up to steady-state operating conditions) from a cold start is proportional to RSM. For the proposed 2nd generation MGT, RSM will be ~ 1.5 kg/kW_E and the thermal time constant is about 2.5 minutes. After warm-up, adjusting r , f , and TIT so that $(T_5 + T_2)$ stays constant over the load range allows extremely rapid response time, determined primarily by the ratio of the rotational kinetic energy of the spindle to the shaft power, which is ~ 1.5 second for a 30 kW_E engine. So after 4-8 minutes of warm-up, the engine's response time from 5-90% power is expected to be ~ 3 seconds. In the 4th-generation MGT, the RSM and thermal time constants drop by a factor of three.

Our experience has shown that the efficient production of MTS recuperators will be rather complex, so it is important to continue to lay some ground work, though we do not plan to devote much effort to recuperator technology during the development of the next generation of advanced MGTs. There are at least five challenging aspects to the high-temperature MTS recuperator production problem: (1) making the headers and spacer grids from an acceptable superalloy; (2) making the superalloy microtubes; (3) automating the assembly of the tube arrays; (4) brazing the headers; and (5) fabricating and assembling the cages and manifolding. Our preliminary investigations and experiments have convinced us that practical solutions can be developed for these challenges when the time comes.

3.8 The Generator and Power Conditioning. There has been dramatic growth in neodymium-boron-iron (Nd-B-Fe) permanent-magnet (PM) machines (mostly motors) over the past eight years in the 1-3000 W range [73]. While their power density (typically 200-800 W/kg) and efficiency (typically 85-94%) appear impressive compared to earlier technology, they still usually operate at rotor surface speeds below 15 m/s and achieve very low performance by the standards

needed for a direct-drive advanced MGT. It seems the highest-power-density generators (or motors) currently available (e.g., for jet-fighter emergency-power generators) above 6 kW achieve only 87% efficiency (at design load) and ~ 1.2 kW/kg (including the housing) at a rotor surface speed of ~ 40 m/s [74], though several groups have demonstrated experimental PM generators above 10 kW with over 94% efficiency and over 95 m/s rotor surface speed.

We and one other company [Hitachi, 75] have demonstrated efficiencies above 97% at rotor surface speeds over 250 m/s [13], which permits over 5 times the power density of the best currently available generators. In both demonstrations, laminated Nd-B-Fe internal PM cylindrical dipole (CD) designs were used with a high-strength rotor sleeve. We used a Si_3N_4 rotor-restraining sleeve (shroud) and quadrature field windings, while Hitachi utilized carbon-fiber rotor wrapping and a more complex field-harmonic-suppression scheme.

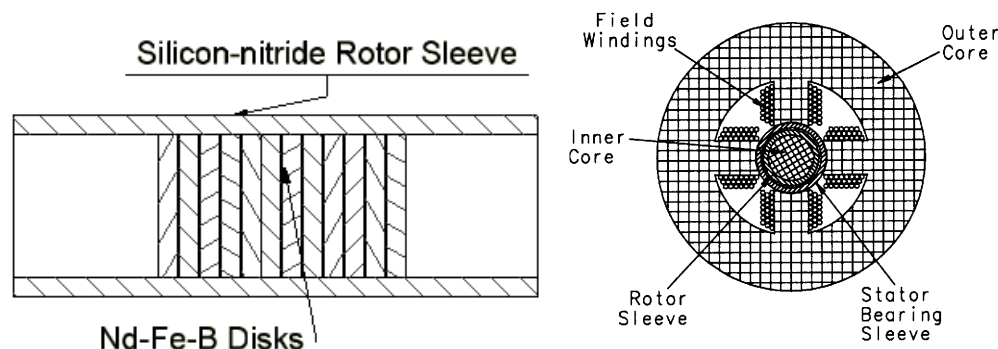


Figure 15. (Left) Laminated cylindrical dipole permanent magnet (CD-PM) generator core.

Figure 16. (Right) Cross-section of the magnetic circuit (not to scale).

**** Our previous experimental apparatus is illustrated schematically in **Figures 15 and 16**. A stack of Nd-B-Fe washers fits snugly inside a silicon-nitride sleeve. The washers are cut from anisotropic material with the orientation axis transverse, and the transverse axes of all washers are aligned in the same direction. The only possible method of assembling this is in the unmagnetized state, but it is not difficult to magnetize them after they are epoxied inside the sleeve with polyimide insulating films and vacuum impregnation. (We have a 7 T, wide-bore, superconducting magnet.) The surprisingly close match in thermal expansion between the Si_3N_4 sleeve and the Nd-B-Fe washers allows our approach to work reliably over a very wide range of temperatures, but the Si_3N_4 sleeve is quite expensive. It appears a hybridization of a restraining method developed by GE [76] and that of Hitachi [75] may be a more cost-effective option. A promising production possibility for the sleeve is carbon-fiber-wrapped stainless, but silicon nitride is probably still preferred for initial experiments.

**** **Of much greater importance than the above manufacturing issue is the need for a high-performance variable-flux generator** to permit high-efficiency constant-voltage output over a wide rpm range. This is essential for the MGT to obtain highest efficiency over a wide range of conditions, as PWM (pulse-width-modulation) voltage transformation will introduce a minimum of an additional 4% loss. There have been prior implementations of variable-flux capability in disk-type generators by varying the axial flux gap, but disk-type machines are not capable of achieving the power density required to match our turbomachinery. The challenges are greater in a cylindrical machine – but not insurmountable. We have recently begun investigating each of the three logical approaches (axial shifts, radial expansion, and azimuthal stator-reluctance control) for the best solution to this problem. Clearly, this is a topic of enormous interest to the automotive industry, where mean generator efficiencies are currently only 45% because of the need to deal with a 10:1 rpm ratio. Our problem is somewhat simplified by the need to accommodate only a 3.5:1 rpm ratio; however, our goal is to obtain 97% generator efficiency over most of the load range. We anticipate the following loss goals can be achieved on the high-power 375 V winding at 60% load: generator winding ohmic losses, 0.5% (even with the rather low power factor from light-weight L-C filters following the rectifiers); stator and rotor core losses, 1%; L-C filter losses, 0.7%; rectifier losses, 0.8%. We anticipate rotor magnet diameters of 20 mm and lengths of 35 mm. We will defer discussion of details until we are further along in the patent process.

Our parametric model of the CD-PM generator will be used to help determine initial design parameters after the expander turbine design is further along. **However, the variable flux/reluctance aspect will require considerable, detailed FEA before going very far. This will be done in collaboration with the Professor Dean Patterson at the Department of Electrical Engineering, University of South Carolina, Columbia.**

**** We conclude here by simply stating that we expect the total mass of our multi-level DC power conditioning system with 97% efficiency to be less than 20 kg for 30 kW power output at several voltages (e.g., 14 VDC, 42 VDC, 115 VDC, and 375 VDC). Only the high-power output voltage will be well-regulated by flux control. Additional regulation can be added to the other voltages at the point of use. Any modest 60 Hz needs are most easily handled using a standard, off-the-shelf, uninterruptible power supply (UPS). The rapid-response of the MGT allows satisfactory operation with a very small battery pack. Note that our system specific mass m_{SS} calculations do not include the storage batteries and assume only DC output power at multiple voltages.

3.9 The Control System. Perhaps the strongest argument for the intercooled cycle is the effective handle it provides for controlling compressor conditions. As inlet temperature decreases below design conditions while TIT is held constant, a simple compressor-restrictor control will cause the compressor to surge, and a simple compressor-bleed control degrades efficiency considerably. Improved off-design performance may be achieved by controlling the cooling flow (i.e., effectiveness) of the intercooler.

**** For efficient system optimization over a wide range of loads and inlet conditions, we expect to depend primarily on (in expected order of significance): fuel flow rate, variable rotational rates on the two stages (i.e., generator fluxes or voltage transformation ratios), adjustable intercooling, variable load balance between the two generators, adjustable inlet guiding vanes on the first-stage compressor, and possibly adjustable outlet flow straightening vanes following the second-stage expander. A control strategy may primarily involve linear interpolation of the control parameters for the desired state between known optimal states from a database of optimal states over the full range of operating conditions of the primary variables – load, inlet temperature, inlet pressure, mean recuperator temperature, and state of charge of the storage battery. Clearly, this involves a lot of detailed simulations to establish the database of optimal states, but it is straightforward. While one could simply ramp slowly (relative to the dominant time constant) when changing states, responsiveness may be enhanced by incorporating a standard PID algorithm, for example. During the Phase I, we will begin to map out the database of optimal states and evaluate several control strategies in more detail in collaboration with Professor Roger Dougal, Department of Electrical Engineering, University of South Carolina.

4.0 Phase I Performance Schedule.

Objective	Tasks	Month #			
	Description	1 - 3	4 - 6	7 - 9	10 - 12
2.1	3.1 System design optimization and software development	X		XXX	X
2.2.1	3.2.3 Design and fabricate ceramic oxidation test rig	X X X			
2.2.1	3.2.3 Evaluate recession in several grades of Si ₃ N ₄ to 1400 K	X	X X X	X	
2.2	3.2.4 CFD, FEA, & erosion optimization of Lu-Si ₃ N ₄ turbine		X X X X		
2.1.3	3.3 CFD optimization of compressor and off-load analysis	X X X			
2.3.1	3.4 Design/fabricate high-speed ball-bearing test apparatus	X X X			
2.3.1	3.4 Evaluate Si ₃ N ₄ ball bearings for wear, stiffness, etc.		X X X	X	X
2.3.2	3.5 Design initial expander demo spindle		X X		
2.3.2	3.5 Fabricate initial demo spindle with titanium turbine		X	X X X	
2.3.3	3.5 Evaluate model spindle at 300 K, 140,000 rpm			X	X X
2.4	3.6 Design and analyze <i>rapid lean micro mix</i> combustor		X X X		
2.5	3.7 Identify candidate vendors of suitable recuperators	X	X X	X	X
2.6	3.8 Preliminary design of variable-flux generator & PC		X X	X	X
2.7	3.9 Preliminary design of control system		X	X X X	X
2.8	4.0 Write Phase I Final Report and Phase II Proposal		X		X X X

5.0 Related Research and Development

As this subject has been largely addressed in the preceding sections and references, only a few additional comments will be made here. Doty Scientific has been developing and producing custom, precision mechanical and RF instruments, primarily for research in Solid State NMR, for 21 years and is the recognized world leader in its specialties (see www.dotynmr.com for more information). Many of these products include air-bearing-supported CFD-optimized micro-turbine-driven silicon-nitride MAS sample spinners capable of achieving supersonic surface speeds and operating at temperatures over the range of 35-1050 K. We have recently begun shipping Magic Angle Spinning (MAS) probes for ultra-high-temperature NMR experiments that utilize diffusion-bonded Lu-Si₃N₄ micro-turbines on gas bearings. Other products include fast-response temperature controllers and high-performance MRI gradient coils. Some of the relevant publications and patents of the Principal Investigator are included in the references, Section 7.

We recently completed an MDA Phase I SBIR study of an advanced MGT for aero-missions. A year ago we completed a Phase II SBIR from DOE, DE-FG02-98ER82565, for work toward the development of a 1 W, 10 K Reverse Brayton Cycle (RBC) cryocooler. Substantial progress was made on the ultra-compact recuperators, micro-turbo-expanders (mass flow rates below 0.3 g/s), helium micro-turbo-compressor design (2.5 g/s helium), and micro-generators. Two NIH Phase I SBIR grants involving the use of ceramic microturbines with gas bearings for MAS NMR applications will soon be completed.

6.0 Commercialization Strategy

Doty Scientific understands the importance of producing real, economically viable products – more than 90% of our revenues have come from the sale of sophisticated products we have manufactured. From a business perspective, one of the more appealing features of this proposed turbogenerator is its scalability and hence potential to succeed in many markets. Clean, efficient, quiet, long-life, light-weight, energy conversion appears possible at output powers from 10 kW to over 500 kW with relatively minor system design changes. Ultimately, we anticipate many mobile applications owing to ultra-low emissions, multi-fuel compatibility, and very high efficiency (refer again to Table 1) with more than an order-of-magnitude off-design load range. We also expect the proposed engine to be much less expensive and less massive than fuel-cell hybrids. Hence, we expect that mid-way through the Phase II, outside investors will be found to adequately support the Phase III. Assuming the timely availability of sufficient Phase III funds, the proposed variable-load 30 kW MGT is expected to be ready for small-scale field testing in about five years. We are projecting the price will be ~\$20,000 each within several years thereafter at moderate production quantities. More details will be presented in the Phase II proposal.

Cost, Reliability, and Safety Issues. With over 20 years of manufacturing and international sales experience, we are keenly aware that cost, reliability, and safety issues must be addressed at all stages. Lifetime, reliability, service, and safety issues will receive high priority, as they affect total ownership cost. Redundant turbine over-speed protection, severe pre-testing, adequate safety margins, and safety shields will eliminate the possibility of injury from rotor failure. The Phase II will include system tests.

System integration issues and manufacturing cost analysis will be important parts of the Phase I study and system design. We expect our 2nd-Generation MGT will be available for premium military and civilian applications in about five years at twice the price (per kW) of advanced diesels. Within a few years thereafter as manufacturing processes mature, we expect it to begin to compete more favorably with established power sources for many land-based mobile applications. While each of the proposed development generations will present challenges, only the progression from 4th to 5th generation seems likely to be beyond the level of effort that one often finds funded in 3-5 year grants to single institutions.

7.0 References

1. S. G. Pouloupoulos, C. J. Philippopoulos, "The effect of Adding Oxygenated Compounds to Gasoline on Automotive Exhaust Emissions," *J. Engr. for Gas Tur. and Power-ASME*, **125**, 1, 344-350, **2003**.
2. T. Itoh, Y. Yoshida, S. Sasaki, M. Sasaki, H. Ogita, "Japanese Automotive Ceramic Gas Turbine Development," in *Ceramic Gas Turbine Design and Test Experience*, ASME Press, NY, **2002**.
3. Bjoern Schenk, "Ceramic Turbine Engine Demonstration Project: A Summary Report," *J. Engr. for Gas Tur. and Power-ASME*, **124**, 3, 617-626, **2002**.
4. R. E. Annati and J. R. Smyth, "Garrett GTP50-1 Multipurpose Small Power Unit...", ASME 91-GT-328, presented at Gas Turb. and Aeroengine Cong., Orlando, **1991**.
5. R. G. Caldwell, et al, "The Ford Turbine ...," SAE paper 720168, 1972. J. C. Napier, "Development of T-100 Multipurpose Small Power Unit," ASME 91-GT-327, 1991. A. W. Court, K. R. Pullen, and C. B. Besant, "Small Gas Turbine Design...", *Proc. Instn. Mech. Engrs.*, 213-A, 339-347, **1999**.
6. A. F. Massardo, C. F. McDonald, T. Korakianitis, "Microturbine/Fuel-Cell Coupling for High-Efficiency Electrical-Power Generation," *J. Engr. for Gas Tur. and Power-ASME*, **124**, 1, 110-116, **2002**.
7. Capstone product literature, <http://www.microturbine.com/>, Chatsworth, CA, **2002**.
8. M. A. White, J. E. Noble, et al, "Preliminary Design of an Advanced Stirling System for Terrestrial Energy Conversion," *Proc.*, Vol. 5, 25th IECEC, Reno; AICE, NY, 1990. W. T. Beale et al, "Prelim. Design of a 7 kW Free-Piston Stirling Engine...", 10th ISEC, Osnabruck, **2001**.
9. Fuel Cell Handbook, 6th edition, US-DOE, Morgantown, W Va, **11/2002**.
10. H. C. Wong, "Laboratory Development of the Enhanced Caterpillar C12 Dual-Fuel Truck Engine," National Renewable Energy Lab Final Report 010043, October, **2001**.
11. M. K. Budlinski, "Heat-Exchanger and Fuel Reformer Technology for PEM Fuel Cells at General Motors," presented at the ASM Materials Solutions Conference, Columbus, OH, **2002**.
12. F. Lofaj, S. M. Wiederhorn, G. G. Long, and P. R. Jemian, "Tensile Creep in Next Generation Si₃N₄," *Proceed.*, 25th Annual Conf. on ...Ceramics..., 167-174, ACS, Cocoa Beach, FL, **2001**.
13. **Arthur Boman, F. D. Doty, J. B. Spitzmesser**, et al, "Development of a 2 W, 10 K Microturbine Cryocooler," Final Report, DOE Grant # FG02-98ER82565, **2001**.
14. M. Y. Leong, C. S. Smugeresky, G. S. Samuelsen, "Rapid Liquid Fuel Mixing for Lean-Burning Combustors: Low-Power Performance," *J. Engr. for Gas Tur. and Power-ASME*, **123**, 3, 574-579, **2001**.
15. A. Schulz, "New Design Principles for Ceramic Hot Gas Components of Gas Turbines," in *Ceramic Gas Turbine Design and Test Experience*, ASME Press, NY, **2002**.
16. W. D. Brentnall, M. van Roode, P. F. Norton, S. Gates... N. Miriyala, "Ceramic Gas Turbine Development at Solar Turbines Inc.," in *Ceramic Gas Turbine Design and Test Exper.*, ASME Press, NY, **2002**.
17. R. Pompe, M. Halvarsson, K. Kishi, and R. Lundberg, "On the Mechanism of High Temperature Strength Degradation of Low-doped HIPed Si₃N₄...", *Proceed.*, 25th Conf....Ceramics..., 183-190, ACS, **2001**.
18. **F. D. Doty**, G. S. Hosford, **J. B. Spitzmesser**, and J. D. Jones, "The Microtube Strip Heat Exchanger," *Heat Transfer Engr.*, 12, 3, 31-41, **1991**.
19. I. Takehara, T. Tatsumi, Y. Ichikawa, "Summary of CGT302 Ceramic Gas Turbine Research and Development Program," *J. Engr. for Gas Tur. and Power-ASME*, **124**, 3, 627-635, **2002**.
20. K. Takase, H. Furukawa, K. Nakano, "A Preliminary Study of an inter-cooled and Recuperative Micro Gas Turbine below 300 kW," ASME-GT-2002-30403.
21. David Gordon Wilson, *The Design of High Efficiency Turbomachinery and Gas Turbines*, MIT Press, Cambridge, 2nd ed. **1996**.
22. A. H. Epstein, S. D. Senturia, et al, "Micro-Heat Engines...The MIT Microengine Project," AIAA 97-1773, 28th AIAA Fluid Dynamics Conf., 1997. A.H. Epstein, S. A. Jacobson, et al, "Shirtbutton-Sized Gas Turbines: The Engineering Challenges...", MIT Gas Turbine Lab, report for U.S. Army and DARPA, **2000**. F. F. Ehrich, S. A. Jacobson, "Development of High-Speed Gas Bearings for ... Micro-devices," *J. Engr. for Gas Tur. and Power-ASME*, **125**, 1, 141-148, **2003**.
23. D. G. Wilson, "Low-leakage and high-flow Regenerators for Gas Turbine Engines," *Proc. Instn. Mech. Engrs.*, 207-A, 195-202, **1993**.
24. Ingersoll-Rand product literature, <http://205.147.212.185/>, **2002**.
25. P. P. Walsh and P. Fletcher, *Gas Turbine Performance*, Blackwell Science, Oxford, UK, **1998**.
26. **F. D. Doty** and J. D. Jones, "A New Look at the Closed Brayton Cycle," *Proceedings IECEC-90*, Vol. 2, Am. Inst. Chem. Engr., NY, 166-172, **1990**.

27. **F. D. Doty** et al, "An Ultra-Compact, Laminar-Flow Cryogenic Heat Exchanger," in *Adv. in Cryo. Engr.*, Vol. 37 A, Plenum Press, NY, 233-240, **1992**.
28. E. Utrianinen and B. Sundén, "Evaluation of the Cross Corrugated and Some Other Heat Transfer Surfaces for Microturbine Recuperators," *J. Engr. for Gas Tur. and Power-ASME*, **124**, 3, 550-560, **2002**.
29. M. Aube and C. Hirsch, GT-0309, "Numerical Investigation of a 1-1/2 Axial Turbine Stage at ... Fully Unsteady Conditions," ASME Turbo Expo **2001**, New Orleans. (Fine/Turbo 5.2, Numeca, Brussels.)
30. **F. D. Doty** and P. D. Ellis, *Rev. Sci. Instrum.*, 52 (12), "Design of High Speed Cylindrical NMR Sample Spinners," 1868-75, **1981**.
31. **F. D. Doty**, B. L. Miller, G. S. Hosford, D. G. Wilson, W. Huanbo, and J. D. Jones, "High Efficiency Microturbine Technology," *Proc., IECEC-91*, 2, 436-442, **1991**.
32. **F. D. Doty**, R. R. Inners, and P. D. Ellis, *J. Mag. Res.*, 43, "A Multinuclear Double Tuned NMR Probe for Applications with Solids...", 399-416, 1981. **F. D. Doty**, "Solid State Probe Design," *Encyclopedia of NMR*, Vol. 7, Wiley, **1996**.
33. **F. D. Doty**, J. B. Spitzmesser, and D. G. Wilson, "High Temperature NMR Sample Spinner," U. S. Patent 5,202,633, 324/321, **1993**.
34. K. Rundgren and O. Lyckfeldt, "Pressing and Sintering Developments in Freeze Granulated Si₃N₄ Materials," Presented at 27th Intern. Confer. on Composites and Adv. Ceramics, Cocoa Beach, FL, **2003**. Also, see product literature, Permascand AB, Ljungaverk, Sweden, **2003**.
35. S. K. Lee et al, "Si₃N₄ Ceramics for...Advanced...Engines," 25th Intern. Confer. on Composites and Adv. Ceramics, Am. Cer. Soc., Cocoa Beach, FL, **2001**.
36. H. T. Lin, S. B. Waters, K. L. More, "Evaluation of Creep Properties of AS800 Si₃N₄," *Proceed.*, 25th Annual Conf. on ...Ceramics..., 175-182, ACS, Cocoa Beach, FL, **2001**.
37. Honeywell, Ceramic Components, product literature, Torrance, CA Jan. **2001**.
38. H. D. Kim, "A Two-step Sintering Process to Obtain Bimodal Microstructures in Si₃N₄," presented at 25th Intern. Confer. on Adv. Ceramics, Cocoa Beach, FL, **2001**.
39. H. Klemm, "Oxidation Behavior of Various Silicon Nitride Materials," presented at 27th Intern. Confer. on Adv. Ceramics, Cocoa Beach, FL, **2003**.
40. K. T. Lin and M. Singh, "Evaluation of Lifetime Performance of Hi-Nicalon Fiber Reinforced Melt-Infiltrated SiC Ceramic Composites," *Advances in SiC/SiC Composites*, Am. Cer. Soc., **2002**.
41. P. S. DiMascio, R. M. Orenstein, M. S. Schroder, L. Tognarelli, G. S. Corman, and A. J. Dean, "General Electric Company," in *Ceramic Gas Turbine Design and Test Experience*, ASME Press, NY, **2002**.
42. T. Hisamatsu, I. Yuri, T. Machida, K. Wada, "Development of Ceramic Gas Turbine for Power Plants," in *Ceramic Gas Turbine Design and Test Experience*, ASME Press, NY, **2002**.
43. I. Tsarenko, H. Du, W. Y. Lee J. Holosczyk, "Effects of Thin CVD-Si Layer on the Oxidation Behavior of Si₃N₄," *Proceed. 26th Intern. Confer. on Comp. and Adv. Ceramics*, B, 497-504, Am. Cer. Soc., **2002**.
44. M. Asayama and A. Motohide (of Fine Ceramics Research Assoc., Nagayo, Japan) "Reaction Bonding of Environmental Coatings on Silicon Nitride," presented at 27th Intern. Confer. on Adv. Ceramics, Cocoa Beach, FL, **2003**.
45. B. Schenk, Honeywell Systems and Service, private communication, **2003**.
46. L. J. Spadaccini, D. R. Sobel, H. Huang, "Deposit Formation and Mitigation in Aircraft Fuels," *J. Engr. for Gas Tur. and Power-ASME*, **123**, 4, 741-746, **2001**.
47. N. Nakazawa, H. Ogita, M. Takahashi, and Y. Mori, "Radial Turbine Development for 100 kW Automotive Ceramic Gas Turbine," ASME paper 96-GT-366, pres. at GT Congress, Birmingham, UK, **1996**.
48. S. R. Choi, J. Pereira, L. A. Janosik, and R. T. Bhatt, "Foreign Object Damage in Disks of Two Gas-Turbine-Grade Silicon Nitrides," pres. at 27th Intern. Confer. on Adv. Ceramics, Cocoa Beach, FL, **2003**.
49. S. Pierret, A. Demeulenaere, B. Gouverneur, C. Hirsch, and R. Van den Braembussche, "Designing Turbomachinery Blades with the Function Approximation Concept and the Navier-Stokes Equations," AIAA/NASA/USAF/ISSMO Symposium on MDO, paper 2000-4879, Long Beach CA, **2000**.
50. H. J. Feld, S. Aschenbrenner, R. Girsberger, "...Acoustic Phenomena at the Inlet... of a Centrifugal Compressor..." GT-0314, ASME Turbo Expo 2001, New Orleans, LA, **2001**.
51. Performance Techniques, Garrett Turbines, www.turbocharged.com/catalog/comp_wheels.html, **2002**.
52. IHI Turbo, product information, http://www.ihit-turbo.com/turbo_RHE-RHF.htm, **2002**.
53. C. Rodgers, "The Efficiencies of Single-Stage Centrifugal Compressors for Aircraft Applications," presented at the GT Congress, Orlando, ASME paper 91-GT-77, **1991**.
54. F. Blanchini, P. Giannattasio, D. Micheli, P. Pinamonti, "Experimental Evaluation of a High-Gain Control for Compressor Surge Suppression," *J. Turbomachinery-ASME*, **124**, 27-35, **2002**.
55. Glenn Research Center, Oil-free Turbomachinery Program, grc.nasa.gov, **2002**.

56. **F. D. Doty**, L. G. Hacker, **J. B. Spitzmesser**, "Supersonic Sample Spinner", US Pat # 5,508,615, **1996**.
57. J. F. Walton II, H. Hesmat, "Application of Foil Bearings to Turbomachinery Including Vertical Operation," *J. Engr. for Gas Tur. and Power-ASME*, **124**, 4, 1032-1041, **2002**.
58. *Superlaminar Flow in Bearings*, ed. by D. Dowson and C. Taylor, MEP, London, 1975.
59. Barden, ceramic ball bearings, <http://www.bardenbearings.com/products.htm>, **2002**.
60. M. J. Donachie, and S. J. Donachie, "*Superalloys, A Technical Guide*," ASM International, **2002**.
61. **F. D. Doty** et al, "A High-Pressure NMR Cell for Biochemical Applications," SBIR Phase I Final Report, NSF Grant # DMI-9560271, **1996**.
62. S. D. Brandi et al, "Brazeability and Solderability of Engineering Materials," in *Metals Handbook, Vol. 6*, ASM International, Materials Part, OH, **1991**.
63. M. M. Schwartz, *Ceramic Joining*, ASM International, Materials Part, OH, **1990**.
64. L. E. Kinsler and A. R. Frey, *Fundamentals of Acoustics*, 2nd ed., Wiley, NY, 1962.
65. D. Y. Yee, K. Lundberg, and C. K. Weakley, "... A 1.5 MW Gas Turbine with a Low Emissions Catalytic Combustion Sys.," *J. Engr. for Gas Tur. and Power-ASME*, **123**, 3, 550-556, **2001**.
66. D. V. Volkov, A. A. Belokin, D. Lyubimov, V. Azkharov, G. Opdyke, "Flamelet Model of NO_x in a Diffusion Flame Combustor," *J. Engr. for Gas Tur. and Power-ASME*, **123**, 4, 774-778, **2001**.
67. C. J. Montgomery, S. M. Cannn, M. A. Mawid, B. Sekar "Reduced Chemical Kinetic Mechanisms for JP-8 Combustion," AIAA paper 2002-0336, presented at 40th Aerospace Meeting, Reno, **2002**.
68. P. J. Maziasz, R. W. Swindeman, B. A. Pint, K. L. More, "Advanced Stainless Steels and Alloys for High-Temperature Recuperators," presented at the ASM Materials Solutions Conf., Columbus, OH, **2002**.
69. P. J. Maziasz, R. W. Swindeman, "Selecting and Developing Advanced Alloys for Creep-Resistance for Microturbine Recuperator Applicaitons," *J. Engr. for Gas Tur. and Power-ASME*, **125**, 1, 310-315, **2003**.
70. **F. D. Doty**, "Microtube-Strip (MTS) Heat Exchanger," U. S. Pat # 4,676,305, **1987**.
71. *Metals Handbook, Vol. 1*, ASM International, Materials Part, OH, **1991**.
72. *Metals Handbook, Vol. 2*, ASM International, Materials Part, OH, **1991**.
73. See product information for Maxon Motor, <http://www.maxonmotorusa.com/>, and Xtreme Energy Inc., <http://www.xtreme-energy.com>, **2002**.
74. Pacific Scientific Electro Kinetics Division, <http://www.psekd.com>, product information, **2002**.
75. H. Koharagi et al, "Very High Permanent Magnet Type ... Rotating Machine...", Hitachi, U.S. Pat. # 6,441,523 B1, **2002**.
76. D. W. Jones, "Method of Applying Containment Shroud on Permanent Magnet Rotors", GE, Schenectady, NY, U.S. Pat. # 4,759,116.

8.0 Principal Investigator and Key Personnel

Principal Investigator: **F. David Doty, Ph. D.**

President - Doty Scientific, Inc. - 1982 to present.

B.A. Physics, Anderson University, Anderson, Ind., 1972, 3.9/4.

Ph.D. Physics, Instrumentation - University of South Carolina, 1983, honors.

David Doty formed Doty Scientific, Inc. while completing graduate school at USC. He has directed all research, development and business activities at DSI for the past 21 years. His professional experiences, publications, and patents span nuclear magnetic resonance, electro-dynamics, turbomachinery, materials science, instrumentation, heat transfer, rf and digital electronics, acoustics, and business management.

1997- 3/00 Member, NIH Center for Scientific Review, Study Section 8, Bioengineering.

1982- Present President, research director, and major owner, Doty Scientific, Inc.

Selected, Federally Funded Research (of 14 total)

1987 PI, SBIR Phase II, "... Class AB Pulse Amplifiers for MRI," NIH #44-CM-77804.

1988 PI, SBIR Phase I, "...Aircraft Surface Heat Transfer," DARPA DAAHO1-88-0761.

1999 PI, SBIR Phase II, "Devel. of a ... 1W, 10 K, RBC Cryocooler," DOE, DE-FG02-98ER82565.

2001 PI, SBIR Phase I, "Devel. of a 50-kHz MAS Probe for ¹H High-Resolution NMR on Insoluble Biomolecules," current Phase I NIH SBIR grant, 1 R43 RR16417-01.

2001 PI, SBIR Phase I, "Devel. of ... Turbo-generators for Aero-missions..." MDA, DASG60-02-P-0199.

2002 PI, SBIR Phase I, "Cryo-coil HR-MAS Probe for improved NMR SNR," current, 1R43EB00152-01.

2002 PI, SBIR Phase II, "High Throughput RF Coils for High-Field MRI," current, 1 R44EB445-02.

Selected research papers and invited presentations (of 35 total; also, see references)

F. D. Doty and P. D. Ellis, *Rev. Sci. Instrum.*, 52 (12), "Design of High Speed Cylindrical NMR Sample Spinners," 1868-1875 (1981).

F. D. Doty, T. J. Connick, X. Z. Ni, and M. N. Clingan, "Noise in High Power, High Frequency Double Tuned Probes," *J. Mag. Res.* 77, 536-549, (1988).

F. D. Doty et al, "High-Performance Class AB Pulse Amplifiers for MRI," Final Report, NIH NCI Contract #N44-CM-77804, (August, 1989).

F. D. Doty, G. S. Hosford, and **J. B. Spitzmesser**, "MTS Heat Exchangers for Space Power", *Trans. Seventh Symp. on Space Nuc. Power Sys.*, Vol. 2, 626-632, NM (1990).

F. D. Doty, G. Hosford, J. D. Jones, and **J. B. Spitzmesser**, *Proceedings, IECEC-90*, "A Laminar Flow Heat Exchanger", 4, 1-7 (1990).

F. D. Doty and J. D. Jones, *Proceedings, IECEC-90*, "A New Look at the Closed Brayton Cycle", 2, 166-172 (1990).

F. D. Doty, G. S. Hosford, **J. B. Spitzmesser**, and J. D. Jones, "The Microtube Strip Heat Exchanger," *Heat Transfer Engr.*, 12, 3, 31-41, 1991.

F. D. Doty, B. L. Miller, G. S. Hosford, D. G. Wilson, W. Huanbo, and J. D. Jones, *Proceedings, IECEC-91*, "High Efficiency Microturbine Technology," 2, 436-442 (1991).

F. D. Doty, G. S. Hosford, **J. B. Spitzmesser**, and J. R. Bittner, "An Ultra-Compact, Laminar-Flow Cryogenic Heat Exchanger", *Adv. in Cry. Engr.*, Vol 37A, 233-240 (1992).

F. D. Doty and L. G. Hacker, "Supersonic Sample Spinners for Solids NMR," Presented at the 34th Rocky Mountain Conference on Analytical Chemistry, Denver, CO, (1992).

- F. D. Doty, "(NMR) Probe Design and Construction," *The Encycl. of NMR Vol. 6*, Wiley, 3753-3762, **1996**.
- F. D. Doty, "Solid State NMR Probe Design," *The Encycl. of NMR Vol. 7*, Wiley, 4475-4485, **1996**.
- F. D. Doty et al, "A Commercial High-Pressure Nuclear Magnetic Resonance Cell for Biochemical Applications," NSF SBIR Phase I Final Report, **1996**.
- F. D. Doty, Y. A. Yang, and G. Entzminger, "Magnetism in NMR Probe Design Part I: General Methods," *Concepts in Magn. Resn.*, Vol 10(3) **1998**, 133-156.
- F. D. Doty, Y. A. Yang, and G. Entzminger, "Magnetism in NMR Probe Design Part II: HR MAS," *Concepts in Magn. Resn.*, Vol 10(4), **1998** 239-260.
- F. D. Doty, "MRI Gradient Coil Optimization", in *Spatially Resolved Magnetic Resonance*, ed. P. Blumler, B. Blumich, R. E. Botto, and E. Fukushima, Wiley-VCH, **1998**.
- F. D. Doty, G. Entzminger, D. McCree, V. Cothran, Laura Holte, S. Klein, "NMR RF Circuit Optimization for Biological Solids at High Fields", Presented at the ENC, Orlando, FL, Mar, **1999**.
- F. D. Doty, George Entzminger, Cory D. Hauck, and John P. Staab, "Practical Aspects of Birdcage Coils", *J. Magn. Reson.*, **1999**, 138:144-154.
- F. D. Doty, George Entzminger, and Cory D. Hauck, "Error-Tolerant Litz Coils for NMR/MRI", *J. Magn. Reson.*, **1999**, 140:17-31.
- F. D. Doty, "MRI Gradient Coil Optimization", Presented at the High-Field MRI Hardware Workshop, Minneapolis, Oct., **1999**.

Selected U.S. Patents (of 35 total; also, see references)

- F. D. Doty, "Microtube-Strip (MTS) Heat Exchanger," 4,676,305, 165/168 (1987).
- F. D. Doty, "Strip-Line-Core Transformers," 4,785,273, 336/61 (1988).
- F. D. Doty, J. B. Spitzmesser, and D. G. Wilson, "High Temperature NMR Sample Spinner," 5,202,633, (1993).
- F. D. Doty, "NMR Sample Rotor Cooling Technique," 5,289,130, 324/321 (1994).
- F. D. Doty, "Double Rotation NMR Sample Spinner," 5,325,059, (1994).
- F. D. Doty, "Doubly Broadband Triple Resonance NMR Probe Circuit," 5,424,645, (1995).
- F. D. Doty, L. G. Hacker, and J.B. Spitzmesser, "Supersonic Sample Spinner," 5,508,615, (1996).
- F. D. Doty and James K. Wilcher, "Crescent Gradient Coils", 5,554,929 (1996).
- F. D. Doty, "Low Inductance Transverse Litz Foil Coils," 6,060,882, (2000).
- F. D. Doty, "Edge-wound RF Solenoid for NMR," 6,087,832, (2000).
- F. D. Doty and Yungan Yang, "HR MAS NMR Coils with Magic Angle Capacitors," 6,130,537, (2000).
- F. D. Doty and G. Entzminger J., "Thermal Buffering of Cross-Coils in High-Power NMR Decoupling," 6,320,384 B1, (2001).

Biographical Information for: JAMIL A. KHAN
Department of Mechanical Engineering, College of Engineering
University of South Carolina, Columbia, SC 29208
Tel: (803) 777-1578; Fax: (803) 777-0106

EDUCATION

Ph.D. Mechanical Engineering, Clemson University, 1988
M.S. Mechanical Engineering, Clemson University, 1984
B.Sc. Mechanical Engineering, Bangladesh Univ. of Engineering & Technology, 1977

AWARDS

- Litman Teaching Award, College of Engineering, USC, 1999 (Highest teaching award of the college, awarded to 1 faculty per year)
- Mungo Teaching Award (University of South Carolina Teaching Award), 1996
- Professor of the Year, Pi Tau Sigma (Mechanical Engineering Honors Society), 1996
- Teacher of the Year, National Society of Black Engineers, 1993
- Best Teacher of the Year, National Society of Black Engineers, 1994
- Lilly Teaching Fellow, University of South Carolina, 1992-93
- Outstanding Graduate Teaching Assistant, Clemson University, 1988

PROFESSIONAL EXPERIENCE

Associate Prof. of Mechanical Engineering, University of South Carolina, August 1996-Present
Assistant Prof. of Mechanical Engineering, University of South Carolina, Aug 1990-July 1996
Assistant Professor, Valdosta State University, Valdosta, GA, September 1988- June 1990
Visiting Assistant Professor, Clemson University, Clemson, SC, June 1989- August 1989
Teaching and Research Assistant, Clemson University, 1982-1988
Licensed Professional Engineer in South Carolina
Member of the American Society of Mechanical Engineers
Member of the American Society of Engineering Education

RESEARCH INTERESTS:

Enhanced heat transfer and heat transfer in reacting flows. Modeling of manufacturing processes, temperature distribution during machining, heat transfer and fluid flow with phase change (solidification/melting in casting, welding), computational and experimental fluid dynamics related to contaminants transport in rooms, heat transfer in porous media, micro-channel heat transfer. Thermodynamic analysis of IC Engines, CFD analysis of combustion processes etc.

PROFESSIONAL SERVICE:

Technical Reviewer for:

J. of Mechanical Engineering Research and Development; Int. Journal of Mass and Heat Transfer; J. of Metallurgical Transactions; J. of Numerical Heat Transfer; AIAA J. Thermo Physics and Heat Transfer; ASME J. of Heat Transfer.

FUNDED RESEARCH:

Had external funding (as either PI or CoPI) for every single year (more than \$5 million). Funding sources: NSF, DoE, NSF/EPSCoR, DHHS/NIOSH, SCUREF, SCHWMF, and Industries. **The following are currently active grants:** a \$ 138,820 grant as PI with Rhodes (SCUREF/DoE); a \$ 341,000 NSF as Co-PI with Reynolds and Deng; a \$ 607, 228 DHHS/NIOSH grant as Co-PI with Feigley; a \$20,000 CMAT grant as PI with M.A. Khan.

SELECTED REFEREED ARTICLES IN PRINT (out of more than 65):

- Fleming, W.H., Khan, J. A., Rhodes, C. A., "Effective Heat Transfer in a Metal-Hydride-Based Hydrogen Separation Process, In *Int. Journal of Hydrogen Energy*, Vol. 26, pp. 711-724, 2001.
- Feigley, C., Bennett, J., Khan, J., Lee, E., "Improving the Use of Mixing Factors for Dilution Ventilation Design" accepted for publication in the *Applied Occupational and Environmental Hygiene Journal*, 2001.
- Khan, J. A., Pohan, A. N., Rhodes, C. A., "Single and Two-Phase Flow Between Two Parallel Micro-Channels: An Experimental Investigation", Accepted for publication in the *Journal of Energy, Heat, and Mass Transfer*, 2002.
- Khan, J.A. Broach, K., and Kabir, A.A.S.A., " Numerical Thermal Model of Resistance Spot Welding in Aluminum," *AIAA Journal of Thermophysics and Heat Transfer*, Vol. 14, No. 1, pp. 88-95, 2000.
- Bennett, J. S., Feigley, C. E., Khan, J.A., and Hosni, M. H. "Comparison of Mathematical Models for Exposure Assessment with Computational Fluid Dynamic Simulation", *J. of Applied Occupational and Environmental Hygiene*, Vol. 15, No. 1, pp. 131-144, 2000.
- Khan, J.A., Xu, L., Chao, Y., and Broach, K. (2000), Numerical Simulation of Resistance Spot Welding Process, *J. of Numerical Heat Transfer*, Part A., Vol. 37, No. 5, pp. 425-446.
- Lijun Xu, Khan, J. A., Zhihang, Chen, "Thermal Load Deviation Model for Superheater and Reheater of a Utility Boiler", in *Journal of Applied Thermal Engineering*, Vol. 20, No.6, pp. 545-558, 2000.
- Khan, J. A., Xu, L, Chao, Y-J., "Nugget Development during Resistance Spot Welding Using A Coupled Thermal-Electrical-Mechanical Model" in the *Journal of Science and Technology of Welding and Joining*, Vol. 4, No.4 , pp.201-207, 1999.
- Hays, A.M., Flora, J.R.V., and Khan, J.A., "Electrolytic Stimulation of Denitrification in Sand Columns-A Research Note" in the *Journal of Water Research*, Vol. 32, No. 9, pp. 2830-1834, 1998.
- Khan, J.A., Fang, Z., and Dutta, S. , "Computational Modeling of Aerosol Particle Transport and Deposition in Abrupt Contraction," in the *Journal of Computer Modeling and Simulation in Engineering*, No.4, Vol. 3, pp. 228-234, Nov. 1998.
- Dutta, S. and Khan, J.A., "Numerical Prediction of Fully Developed Rotating Channel Flow with Modified Two-Equation Turbulence Model," accepted to the *Journal of Mechanical Engineering Research and Development*, Vol. 20-21, pp. 53-70, 1999.
- Lijun Xu and Khan, J.A, Nugget Growth Model for Al-Alloys During Resistance Spot Welding, in *Welding Journal*, Vol. 78, No. 11, pp. 367-s to 372-s, 1999.**
- Dutta, S., Zhang, X., Khan, J., and Bell, D. (1999), "Adverse and Favorable Mixed Convection Heat Transfer in a Two-sided Heated Square Channel." in the *Journal of Experimental Thermal and Fluid Science*, vol. 18, pp. 314-322, 1999.
- Khan, J.A. and Tong, X., " Unidirectional Infiltration and Solidification/Remelting of Al-Cu Alloy," *AIAA Journal of Thermophysics and Heat Transfer*, Vol. 12, No. 1, pp. 100-106, 1998.
- Dutta, S., Dutta, P., Jones, R.E., and Khan, J.A. (1998), "Heat Transfer Coefficient Enhancement with Perforated Baffles," *ASME Journal of Heat Transfer*, Vol. 120, No.3, pp795-797, 1998.
- Dutta, S., Morehouse, J.H., and Khan, J.A. (1997), "Numerical Analysis of Laminar Flow and Heat Transfer in a High Temperature Electrolyzer," *International Journal of Hydrogen Energy* Vol. 22, No. 9, pp. 883-895.
- Mitra, S. A., Acosta, G.M., Khan, J. A., and Smith, R.L., "Extraction of Zinc Oxide from Electric Arc Furnace Dust and Zinc Oxide in Aqueous Ammonium Chloride Solutions from 303-363K," in *Journal of Environmental and Health Science* Vol. A32, No. 2, pp. 497-515, 1997.
- Amin, M.R.and Khan, J.A., "Effects of Multiple Obstructions on Conjugate Forced Convection Heat Transfer,," in *Journal of Numerical Heat Transfer*, Part A, Vol. 29, pp. 265-279, 1996.
- Tong, X. and Khan, J. A., "Infiltration and Solidification/Remelting of Pure Metal in a Porous Preform," *ASME Journal of Heat Transfer*, Vol. 118, pp. 173-180, Feb., 1996.
- Tong, X. and Khan, J.A., Amin, M.R., "Enhancement of Heat Transfer by Inserting A Metal Matrix into A Phase Change Material," *Journal of Numerical Heat Transfer*, Part A, Vol. 30, PP. 125-141, 1996.
- Lee, S.F., Maskalenko, E., Acosta, G.M., Khan, J.A., and Smith, R.L., "Separation of Copper from Plastic Waste Material by Air Classification and Water Flotation," in *Journal of Environmental and Health Science*, Vol. A31, No. 5, pp. 1197-1214, 1996.
- Slater, S. A., Khan, J. A., and Smith, R. L., "Transferring Waste Minimization Solutions Between Industrial Categories With a Unit Operations Approach-- I. Chemical and Plating Industries," *Journal of Environmental and Health Science*, Vol. 30, No. 2, pp. 379-406, 1995.

- Morse, J. S., Khan, J., Caldwell, M., Baxter, S., Drake, B. D., and Smith, R. L., "A Unit Operation Approach to Waste Minimization," *Journal of Environmental and Health Science* Vol. 29. No. 7, pp. 1471-1489, August 1, 1994.
- Yao, G-F. and Khan, J. A., "A Numerical Study of Two-Dimensional High Rayleigh Number Natural Convection Between Two Reservoirs Connected by a Horizontal Duct" *ASME Journal of Heat Transfer*, Vol. 115, No. 3, pp. 800-803, 1993.
- Khan, J. A. and Yao, G-F., "Comparison of Natural Convection of Water and Air in a Partitioned Rectangular Enclosure" in *Int. J. Heat & Mass Transfer*, Vol. 36, No. 12, pp. 3107-3117, 1993.
- Khan, J. A., Pal, D., and Morse, J. S., "Numerical Modeling of a Rotary Kiln Incinerator," *Journal of Hazardous Waste and Hazardous Materials*, Vol. 10, No. 1, pp 81-95, 1993.
- Khan, J. A. and Morehouse, J. H., "A Metal Matrix for Heat Transfer Enhancement During Phase-Change Processes," *Transactions of ASHRAE*, Vol. 100, part II, pp. 707-714, 1994.
- Khan, J. A., Beasley, D. E., and Alatas, B., "Evaporation From a Packed Bed of Porous Particles Into Superheated Vapor," *Int. J. of Heat and Mass Transfer*, Vol 34, No. 1, pp 267-280, 1991.
- Khan, J. A. and Kumar, R., "Natural Convection in Vertical Annuli: A Numerical Study for Constant Heat Flux Inner Wall," in *ASME Journal of Heat Transfer*, Vol 111, pp 909-915, 1989.
- Khan, J. A. and Beasley, D. E., "Two-dimensional Effects on the Transient Response of a Packed Bed Regenerator," *ASME Journal of Heat Transfer*, Vol. 111, No. 2, pp 328-336, 1989.

GRADUATE STUDENTS: 2 post doctoral researchers, 1 Ph.D, 18 MS and **currently** advising 5 Ph.D. and 4 M.S students.

Other Personnel: John Staab, Electrical Engineer

Chief Engineer - Doty Scientific - 1994 to present

Education

1993 MSEE Univ. of Arizona, *summa cum laude*

1991 BSEE, BSMath, Univ. of Wisconsin - Platteville, *summa cum laude*

Areas of expertise include rf electronics, microprocessor control, communications, optics, ceramic micro-turbines for NMR MAS probes, mechanical design, generator design, and manufacturing.

F. D. Doty, Cory D. Hauck, G. Entzminger, and **J. P. Staab**, "Practical Aspects of Birdcage Coils", *J. Magn. Reson.*, **1999**, 138, 144-154.

Arthur Boman, Mechanical Engineer

Education

1994 BSME Univ. of Pittsburgh, *magna cum laude*

Experience

1996 to present Mechanical Engineer, Doty Scientific

1994 - 1995 Mechanical Engineer, Westinghouse, Columbia, SC

Chief engineer on DOE SBIR Phase II, "Develop. of a 1 W 10 K RBC Cryocooler", 1999. Responsible for much of the experimental design, analysis, and documentation.

Areas of expertise include classical stress and vibration analysis, FEA, fluid dynamics, CFD, nuclear power plant operation, heat transfer, CNC manufacturing, NMR probe design, and cryogenics.

Arthur Boman, F.D. Doty, "Design and Manufacture of Ultra-low-mass, Cryogenic Heat Exchangers," *Cryogenics*, **41**, 797-803, 2002.

Jonathan B. Spitzmesser

Senior Manufacturing Engineer - Doty Scientific, Inc. - 1982 to present

Shop Supervisor- G&G Welding and Machine, Columbia SC - 1976 to 1982

J.B. Spitzmesser has been with Doty Scientific, Inc. since its inception and is co-inventor on five patents. He has been responsible for the production of most DSI prototypes and has directed the manufacturing. He has extensive manufacturing and fabricating experience, including vacuum brazing, torch brazing, TIG welding, MIG welding, plasma arc welding, precision machining, CNC machining, diamond grinding, forging, and die design. His numerous design and manufacturing projects include high speed ceramic spinners, MTS heat exchangers, NMR probes, and MRI gradient coil manufacture.

Siddarth Shevgoor, Manufacturing Engineer

Education

2003 MSME, *summa cum laude*, University of Missouri, Rolla, MO

Thesis: "Delamination-free Drilling or Boron/Epoxy Composite Plates"

1998 BSME Highest Honors, Manipal Institute of Technology, India

Development of a semi-direct fuel injection system for small two-stroke engines.

Areas of expertise include CAM/CNC manufacturing, FEA stress analysis, cutting theory, vibrational analysis, compressible flow, shock waves, and fuel injection systems.

Experience:

2/2003 to present Manufacturing Engineer, Doty Scientific

9/1998-8/2000 Mechanical Engr., Bosch Powertrain Systems, Bangalore, India.

Publication:

A. Chukwujekwu and **S. Shevgoor**, "Delamination-free Drilling or Boron/Epoxy Composite Plates", to be submitted.

Santosh Kini, Mechanical Engineer

Education

- 2001 MSME, *summa cum laude*, Ohio State University, Columbus, OH
Thesis: "The Development of Steady State Rotor Wakes"
1999 BSME High Honors, Regional Engineering College, Tiruchirapali, India
Thesis: "Emission control Using a Catalytic Converter"

Areas of expertise include vibrational analysis, compressible flow, computational fluid dynamics, rotating wing analysis, CNC manufacturing, heat transfer, viscous flow, catalysis, and boundary value problems.

VISA: S. Kini holds an H1B visa from India. He will be doing turbine CFD and CNC manufacturing.

Experience: 9/2001-present, Mechanical Engineer, Doty Scientific Inc.

Publications & Presentations

- Santosh Kini and A. T. Conlisk, "The Development of Steady State Rotor Wakes," Aeromechanics Specialist Meeting, American Helicopter Society, Atlanta, GA, 2000.
Santosh Kini, "The Formation of Rotor Tip-Vortices," American Physical Soc., Division of Fluid Dynamics, Washington DC, 2000.

Dr. Laura Holte, Chemist/Bio-Physicist

Education

- 1992 Ph.D. Analytical Chemistry, Honors, Montana State Univ., Bozeman, Montana
1986 B.S. Chemistry, Honors, Mankato State Univ., Mankato, MN
American Institute of Chemists Outstanding Senior Award

Experience

- 1998-2000 NMR/MRI Instruments Sales Manager, Doty Scientific.
1993-1998 NIH Post Doct. Research Fellow, Membrane Biochemistry and Biophysics
1996 Research Associateship Award, National Research Council

Selected Journal Publication (of 8 total)

- L. L. Holte and K. Gawrisch, "Determining Ethanol Distribution in Phospholipid Multilayers with MAS-NOESY spectra," *Biochemistry*, **1997**, 36:4669-4674.

9.0 Facilities/Equipment

Doty Scientific, Inc. operates from a 20,000 ft² facility on a 10-acre site in an industrial park in Columbia, South Carolina. This plant contains all the equipment required for this SBIR project through Phase III, including the following:

Super-precision Ceramics Machining: two Hardinge-618 Lathes - ± 1.5 μm , ID and OD; Sunnen Precision Honing Machine - ± 1.0 μm ID; four Dumore Tool-Post Grinders; Diamond drilling (core, point, and jig trepanning); 50 W cw (15 kW pulse) Nb-YAG laser.

Precision metal, composites, and plastics machining: Takahashi TNC-LO 2 axes CNC; Dahlih MCV-611 4 axes CNC; Five more milling machines and nine lathes.

Oven Brazing and Annealing: Centorr M60 7x16cm oven (1900°C, 20 kW, rapid cycle capability, pressurized nitrogen or inert gas atmosphere, vacuum); custom high-vacuum oven, 0.02 mTorr, to 950°C, 1.5 m x 0.08 m dia.; custom 1050°C, 0.4 m x 0.12 m dia. muffle vacuum furnace, 1 mTorr; 1300°C heat treat furnace; 4 ft³, 550°C oven, etc.

Computer hardware and software: Numeca CFD, BladeGenPlus CFD, Ansoft HFSS, IDEAS 7.0, CAD, CAM, FEA, Inventor, ARRL, Mathematica, etc. Advanced, proprietary magnetic modeling capabilities. Single and dual-processor Pentium-IV workstations up to 2200 MHz. Two dozen smaller computers.

RF electronics and instrument production: Spectrum analyzers, network analyzers, sweep generators, RF scopes to 1.6 GHz, 1 kW broadband VHF/UHF power amps, etc.

Chemistry: Noble metal plating, wet lab, printed circuit etching lab, etc.

NMR: Varian VXR-S 300 MHz Two-Channel Spectrometer; 7 T Wide-Bore Magnet.

Adequate excess manufacturing and engineering capacity is available. If awarded, this contract will be given adequate priority to ensure machine and operator availability.

10.0 Consultants and Subcontractors

Three professors from the University of South Carolina (USC) will collaborate with Doty Scientific. An agreement is on file. CVs and commitment letters will be provided upon request.

Prof. Jamil Kahn, Department of Mechanical Engineering, USC, and a graduate student, will improve and validate the software for evaluating the effects of various system parameters on system efficiency. They will also assist in evaluating candidate recuperators. In addition, their research will explore various designs for rapid fuel-air mixing for "near-zero-emissions" combustion in the autoignition regime using CFD to study the reaction kinetics and species transport. One objective of this study will be to determine an optimum combustor design.

Prof. Roger Dougal, Department of Electrical Engineering, USC, and a graduate student will investigate the scope of simulations required to define and test control strategies for advanced microturbine power sources. The investigation will identify the component models needed for accurate system-level simulations, catalog those that are already available within the VTB environment, and define the scope of new models that are needed to complete a naturally-coupled system model of the turbine power plant. Furthermore, the work will develop preliminary models of the gas turbine system in signal-flow form and begin to design and test specific control strategies including PID and Synergetic.

Prof. Dean Patterson, Department of Electrical Engineering, USC, and one graduate student will explore novel variable-flux, variable speed, constant-voltage permanent magnet generator concepts and conduct detailed finite element analysis of candidate designs.

11.0 Other Grant Applications, Proposals, or Awards.

- A Phase II Grant (DOE DE-FG02-98ER82565), "Development of 1-10 W, 10 K Reverse Brayton Cycle Cryocoolers", was completed a year ago. PI: F. D. Doty. DOE Project officer: Carl Friesen, Argonne, IL. Awarded June 15, 1999. Funding ended June 15, 2001. No overlap.
- A Phase I SBIR grant, 1 R43 RR16417-01, for the development of a 50 kHz ¹H NMR MAS probe was awarded 8/01. PI: F. D. Doty. No overlap.
- A Phase I SBIR grant, R43 NS41127-01, for the development of an MRI head gradient coil, was awarded 5/01 by NIH. PI: F. D. Doty. A Phase II proposal has been submitted. No overlap.
- A Phase I SBIR proposal, 1 R43 EB00152-01, for the development of a cryo-coil MAS probe for improved SNR was awarded 5/02. PI: F. D. Doty. No overlap.
- A Phase I SBIR contract, DASG60-02-P-0199, was awarded (4/02-10/02) by MDA for the preliminary design of an Auxiliary Power Unit for operation at altitudes of 7-14 km.
- A Phase II SBIR grant, NIH NIBIB grant # R44 EB445-02, for the development of advanced MRI RF imaging coils, was awarded 8/02. PI: F. D. Doty. No overlap.
- A Phase I SBIR grant is expected to be awarded soon by NIH for the development of a Narrow Bore SAS NMR Probe for Structure Elucidation in Proteins. PI: F. D. Doty. No overlap.
- A Phase I SBIR proposal was submitted 1/6/03 to Air Force (AF03-292) for the development of a 15 kW GenSet for the MHU-83 mobile bomb-jammer platform. PI: F. D. Doty.
- A Phase I SBIR proposal was submitted 1/10/03 to Air Force (AF03-161) for the development of a 40 kW Emergency Power Unit for the F-16. PI: F. D. Doty.

There are no other current or pending proposals.